Title	Thromboxane A2 synthase inhibitors prevent production of infectious hepatitis C virus in mice with humanized livers.
Author(s)	Abe, Yuichi; Aly, Hussein Hassan; Hiraga, Nobuhiko; Imamura, Michio; Wakita, Takaji; Shimotohno, Kunitada; Chayama, Kazuaki; Hijikata, Makoto
Citation	Gastroenterology (2013), 145(3): 658-667.e11
Issue Date	2013-09
URL	http://hdl.handle.net/2433/178751
Right	© 2013 AGA Institute. Published by Elsevier Inc.
Type	Journal Article
Textversion	author

Thromboxane A2 Synthase Inhibitors Prevent Production of Infectious Hepatitis C Virus in Mice with Humanized Livers

Short title: Prostanoid signals as anti-HCV targets

Authors:

Yuichi Abe[1, 2)], Hussein Hassan Aly[1, 6)], Nobuhiko Hiraga[3)], Michio Imamura[3)], Takaji Wakita[4)], Kunitada Shimotohno[5)], Kazuaki Chayama[3)], Makoto Hijikata[1, 2)]

1) Institute of Virus Research, Kyoto University

2) Graduate School of Biostudies, Kyoto University

3) Department of Gastroenterology and Metabolism, Applied Life Sciences, Institute of Biomedical and Health Sciences, Hiroshima University

4) Department of Virology 2, National Institute of Infectious Disease

5) Research Institute, Chiba Institute of Technology

6) Present address: Department of Virology 2, National Institute of Infectious Disease

Grant support:

This work was supported by grants-in-aid from the Ministry of Health, Labour and Welfare of Japan.

Abbreviations: 2D, two dimensional; 3D, three dimensional; AAC, arachidonic acid cascade; bbHCV, blood-borne HCV; COX, cyclooxygenase; DAA, direct-acting anti-

viral agents; DAPI, 4',6-diamidino-2-phenylindole; DMEM, Dulbecco's modified Eagle's medium; FBS, fetal bovine serum; FITC, fluorescein isothiocyanate; HCVcc, HCV from cell culture; IHH, immortalized human hepatocytes; IP, prostaglandin I_2 receptor; LD, lipid droplet; peg-IFN, polyethylene glycol–conjugated interferon; PHH, Primary human hepatocytes; PGIS, prostaglandin I_2 synthase; RT-PCR, reverse transcriptase polymerase chain reaction; qRT-PCR, quantitative reverse transcriptase polymerase chain reaction; siRNA, small interfering RNA; TP, thromboxane A_2 receptor; TX, thromboxane; TXAS, thromboxane A_2 synthase; TXB_2, thromboxane B_2; uPA/SCID, urokinase plasminogen activator/severe combined immunodeficiency.

Correspondence Makoto Hijikata, PhD

Laboratory of Human Tumor Viruses, Department of Viral Oncology, Institute for Virus Research, Kyoto University

53, Kawaharacho, Shogoin, Sakyoku, Kyoto, 606-8507, Japan

Tel. 81-75-751-4046

FAX 81-75-751-3998

e-mail: mhijikat@virus.kyoto-u.ac.jp

Conflicts of interests: The authors disclose no conflicts

Transcript Profiling: The microarray data in this study was named as "HuSE2, 2Dvs3D", and registered in ArrayExpress. The accession number is E-MTAB-1491.

Nucleic acid sequences: Sequencing data in this study were named as "BankIt1626925 Seq1", "BankIt1626925 Seq3", and registered with GenBank. The accession numbers are KF006982 and KF006984, respectively.

Author Contributions: Yuichi Abe was responsible for study concept and design, acquisition of data, analysis and interpretation of data, drafting of the manuscript, and statistical analysis. Hussein Hassan Aly, and Nobuhiko Hiraga, Michio Imamura were responsible for acquisition of data, and analysis and interpretation of data. Takaji Wakita, Kunitada Shimotohno, and Kazuaki Chayama were responsible for critical revision of the manuscript for important intellectual content and administrative, technical, or material support. Makoto Hijikata was responsible for study concept and design, analysis and interpretation, drafting of the manuscript, critical revision of the manuscript for important intellectual content, obtained funding, and study supervision.

Acknowledgements: The authors thank the following investigator and companies: Dr. Michinori Kohara (Tokyo Metropolitan Institute of Medical Science, Tokyo, Japan) for providing anti-HCV Core antibody; TOYOBO Co. (Osaka, Japan) for providing Hollow fibers; Toray Co. (Tokyo, Japan) for providing Beraprost; Dr. Masayoshi Fukasawa (National Institute of Infectious Disease, Tokyo, Japan) for helpful discussion.

Abstract:

Background & Aims: A 3-dimensional (3D) culture system for immortalized human hepatocytes (HuS-E/2 cells) was recently shown to support the lifecycle of blood-borne hepatitis C virus (HCV). We used this system to identify proteins that are active during the HCV lifecycle under 3D culture conditions.

Methods: We compared gene expression profiles of HuS-E/2 cells cultured under 2D and 3D conditions. We identified signaling pathways that were differentially activated in the cells, and analyzed their functions in the HCV lifecycle using a recombinant HCV-producing cell culture system, with small interfering (si)RNAs and chemical reagents. We investigated the effects of anti-HCV reagents that altered these signaling pathways in mice with humanized livers (carrying human hepatocytes).

Results: Microarray analysis showed that cells cultured under 2D vs 3D conditions expressed different levels of mRNAs encoding prostaglandin synthases. siRNA-mediated knockdown of thromboxane A2 synthase (TXAS) and incubation of hepatocytes with a TXAS inhibitor showed that this enzyme is required for production of infectious HCV, but does not affect replication of the HCV replication or particle release. The TXAS inhibitor and a prostaglandin I2 receptor agonist, which has effects that are opposite those of TXA2, reduced serum levels of HCV and inhibited the infection of human hepatocytes by blood-borne HCV in mice.

Conclusions: An inhibitor of the prostaglandin synthase TXAS inhibits production of infectious HCV particles in cultured hepatocytes and HCV

infection of hepatocytes in mice with humanized livers. It might therefore be developed as therapeutic for HCV infection.

Keywords: infectious virus particle; lipid mediator; antiviral drug

Introduction

Approximately 170 million people worldwide are infected with hepatitis C virus (HCV)[1], with the majority suffering from chronic hepatitis, liver cirrhosis, and/or hepatocellular carcinoma[2]. HCV is currently treated using a combination of polyethylene glycol–conjugated interferon (peg-IFN) and ribavirin, although no more than 60% of individuals adequately respond[3]. Recently, inhibitors of HCV nonstructural proteins have been developed as direct-acting anti-viral agents (DAA) to treat HCV effectively[4-6]. However, HCV often acquires the resistance against the treatment with DAA in case of monotherapy[7]. Current efforts are therefore focused on better understanding the lifecycle of HCV to find the cellular target of novel anti-HCV drug to use the various therapeutic options.

A cell culture system that allows the production of recombinant infectious HCV, called HCVcc, was recently developed using a cloned HCV genome and the hepatocellular carcinoma–derived Huh-7 cell line[8-10]. Experiments using the culture system have provided novel insights on the HCV lifecycle such as finding the production of infectious HCV particles near lipid droplets (LDs) and endoplasmic reticulum–derived LD-associated membranes[11]. Huh-7 cells, however, only allow the proliferation of recombinant HCV, and not blood-borne HCV (bbHCV).

To study the lifecycle of bbHCV, we cloned immortalized human hepatocyte (IHH), HuS-E/2 cells, which permitted some degree of bbHCV infection[12]. Integrating hollow fibers into the three-dimensional (3D) culture system resulted in efficient continuous proliferation of infected HCV production from the cells[13].

Using the improved system, we previously compared the gene expression profiles of HuS-E/2 cells under the 2D and 3D culture conditions using microarray analysis. This allowed us to identify signaling pathways that contribute to the proliferation of HCV, for example, peroxisome proliferator–activated receptor α signaling that enhances HCV replication[14]. This result was confirmed by other groups[15, 16], corroborating that our strategy can uncover cellular events that support the proliferation of HCV. We, therefore, hypothesized that leveraging the *in vitro* systems described above may help elucidate the molecular mechanisms underlying the HCV lifecycle.

Prostanoids are metabolites of the arachidonic acid cascade (AAC) that possess various physiologic activities[17]. These metabolites include prostaglandin (PG) E_2, D_2, I_2, and F_2, and thromboxane A_2 (TXA_2)[17]. Although several studies have shown that PG signaling contributes to liver regeneration[18, 19], the physiologic functions of these lipid mediators in human hepatocytes are still unknown. Interestingly, one report showed that PGE_2 might support HCV genome replication in cells bearing self-replicating HCV subgenomic replicon RNA[20]. Whether prostanoids are involved in the HCV lifecycle, however, has not been precisely investigated.

In this study, we provide evidence that TXA_2 synthase (TXAS) is involved in the formation of infectious HCV, by cell culture system, and that a TXAS inhibitor and PGI_2 receptor (IP) agonist that has opposite physiological effects to TXA_2 can be used as novel anti-HCV drugs, by using chimeric mice bearing transplanted human hepatocytes[21]. This is the first report showing the

contribution of the AAC to HCV infectivity and the potency of a prostanoid as an anti-viral agent.

Materials and Methods.

Cell culture

The human hepatocellular carcinoma–derived Huh-7 and Huh-7.5 cell lines were cultured as described previously[22]. HuS-E/2 cells are IHH transduced with E6 and E7 genes of human papilloma virus 18 and human telomerase reverse transcriptase gene as described previously[12]. 2D and 3D culture conditions for HuS-E/2 cells were as described previously[12].

Reagents and antibodies

FR122047, PGH_2, ONO1301, daltroban, and dibutyryl cyclic adenosine monophosphate (cAMP) sodium salt were purchased from Sigma-Aldrich (Missouri, USA). Cyclooxygenase (COX)-2 inhibitor 1 and Ozagrel were purchased from Santa Cruz Biotechnology (California, USA). U-46619 was purchased from Cayman Chemical (Michigan, USA). Beraprost was a generous gift from Toray Co. (Tokyo, Japan). FR122047, PGH_2, ONO1301, Daltroban, COX-2 inhibitor1, Ozagrel, Beraprost, and Calucium ionophore were dissolved in DMSO. U-46619 and TXB_2 were dissolved in methyl acetate. Dibutyryl cAMP was dissolved in water. The effect of each reagent on cell viability was analyzed using a Cell Proliferation Kit 2 (Roche, Basel, Switzerland) based on the manufacturer's instruction. An antibody specific for Core protein (antibody 32-1) was a gift from Dr. Michinori Kohara (Tokyo Metropolitan Institute of Medical Science, Tokyo, Japan). Rabbit polyclonal anti-NS5A protein CL1 antibody and anti-HCV protein antibody in human serum were described previously[11].

Microarray analysis

Total RNA purified from HuS-E/2 cells cultured under 2D or 3D conditions in the absence of HCV infection was analyzed with a 3D-Gene human chip 25k (Toray, Tokyo, Japan) to compare gene expression profiles as described previously[14]. The accession number of the results is as “E-MTAB-1491” in ArrayExpress.

Production of HCVcc and sample preparation

HCVcc was produced from the Huh-7 or Huh-7.5 cells transfected with *in vitro* synthesized JFH1^{E2FL} or J6/JFH1 RNA as described previously[11]. The transfected cells and culture medium were harvested at four days post-transfection. For JFH1^{E2FL} RNA-transfected Huh-7 cells treated with TXAS-specific small interfering RNA (siRNA), cells and culture medium were harvested at 3 days post-transfection. Culture medium including HCVcc was concentrated used for infection experiments as described previously[11]. Concentrated culture medium from JFH1 RNA-transfected Huh-7 cells was fractionated as described previously[11]. Infectivity titer in each fraction was analyzed by focus-formation assay, which was determined by the average number of HCV-positive foci.

Reverse transcriptase polymerase chain reaction (RT-PCR) and quantitative RT-PCR (qRT-PCR)

Total RNA was isolated from the cells and medium using Sepasol I Super and Sepasol II (Nacalai Tesque), respectively, according to the manufacturer's instructions. Using 200 ng of total RNA as a template, we performed RT-PCR and qRT-PCR with a one-step RNA PCR kit and one-step SYBR Primescript RT-PCR kit 2 (Takara, Shiga, Japan), respectively, according to the manufacturer's instructions. Information on both experiments was shown in Supplemental Table 1 and 2.

Infection of HCVcc

Infection experiment of HCVcc and detection of infected Huh-7.5 cells by indirect immunofluorescence analysis were performed mainly as described previously[11]. The number of infection positive cells detected in 4 x 10^4 target cells one day after infection with HCVcc including 10^7 copies of RNase resistant HCV genome was defined as the specific infectivity in the infection experiments in our protocol.

Indirect immunofluorescence analysis

HCV proteins were examined in cells using a Leica SP2 confocal microscope (Leica, Heidelberg, Germany) and infected cells were counted using a BioZero fluorescence microscope (Keyence, Tokyo, Japan).

Preparation of intracellular HCV particles

Intracellular HCV particles were prepared as described previously[23]

Pharmacological test in chimeric mice bearing transplanted human hepatocytes

All mouse studies were conducted at Hiroshima University and accorded with the guidelines of the local committee for animal experiments. Chimeric mice transplanted with human hepatocytes were generated as described previously[21]. The experimental protocol was approved by the Ethics Review Committee for Animal Experimentation of the Graduate School of Biomedical Sciences (Hiroshima University). The reagents were first administered 1 week after the chimeric mice were infected with 1.0 x 10^5 titer of bbHCV. ONO1301 was injected subcutaneously at a dose of 200 μg per mouse. Beraprost and Ozagrel were orally administrated at a dose of 10 μg and 300 μg per mouse, respectively. For positive control experiment, Telaprevir was administrated as described previously[24]. All reagents were administrated twice each day. Serum samples were collected at 2, 3, and 4 weeks after starting the treatments. HCV RNA levels in the samples were evaluated in quantitative RT-PCRs.

Statistical Analyses of Data

The significance of differences in the means was determined by Student's t test or Wilcoxon signed-rank test (Fig. 7 and Supplemental Fig. 14).

Results

Expression of PG synthase mRNA in HuS-E/2 cells cultured under 3D conditions

To identify signaling pathways that contribute to HCV proliferation under the 3D culture conditions, we compared the gene expression profiles of 2D- and 3D-cultured HuS-E/2 cells as described previously[14]. We found that the expression of 984 genes was up-regulated more than two times in both of two types of 3D-cultured HuS-E/2 cells, and that of 1491 genes was down-regulated less than half time. For the two 3D conditions, we identified the expression of a set of genes encoding enzymes of the AAC. The expression levels of mRNAs for AAC enzymes, COX1, PGD_2 synthase, and TXAS increased in HuS-E/2 cells cultured under the 3D conditions (Fig. 1A), while those for PGE_2 and PGI_2 synthases (PGIS) decreased (Fig. 1A). These results were confirmed by qRT-PCR analysis (Fig. 1A, gray bars). The relative protein levels of those enzymes in 2D and 3D cultured HuS-E/2 cells reflected the quantitative difference of those mRNAs, except PGDS (Fig. 1B). The expression of those genes and the production of those proteins were also observed in the liver tissues from patients with hepatitis C, suggesting the functional roles of those products in the human liver (Supplemental Fig. 1).

The AAC contributes to infectious HCV production

To assess whether the AAC plays roles in the HCV lifecycle, the contributions of the AAC rate-limiting enzymes COX1 and COX2 were examined using the JFH1 cell culture system. We first investigated the role of COX1, of which gene is

known to be a constitutively expressed in general, by adding the COX1 inhibitor FR122047 to JFH1 RNA–transfected cell cultures. Even at the higher concentrations, FR122047 did not markedly affect the amount of HCV RNA in the medium or cells (Fig. 2A, black and white bars) with a little cytotoxicity at 10 μM. Nevertheless, FR122047 dose-dependently decreased the infectivity of HCVcc in the culture medium (Fig. 2B, C). As the infection experiment using lower titer of HCVcc from inhibitor treated cells showed that the inhibitor affected the number of infection positive focus but not the number of the cells in a focus (Fig. 2C), the treatment of COX1 inhibitor seemed to decrease the focus-forming ability of HCVcc. Next, the contribution of inducible COX2 was examined using COX2 inhibitor 1. The inhibitor, however, did not affect the infectivity of HCVcc in the medium (Supplemental Fig. 2A, B), probably because of the lack of COX2 gene expression in Huh-7 cells (Supplemental Fig. 2C and 3A). These data suggested that COX1 and the AAC play a role in infectious HCVcc production without significant effects on HCV genome replication or particle release from the cells.

TXAS plays a key role in infectious HCV production

To further examine the contribution of the AAC to infectious HCVcc production, we focused on TXAS, because, like COX1 mRNA, TXAS mRNA levels increased in HuS-E/2 cells cultured under 3D conditions. Although PGD_2 synthase mRNA levels also increased, this synthase was unlikely to contribute to these processes because we did not detect PGD_2 synthase mRNA in Huh-7

cells in the JFH1 cell culture system (Supplemental Fig. 3A). Using siRNA- and shRNA-mediated suppression of mRNA expression, we found that reducing TXAS mRNA levels in HCVcc-producing Huh-7 cells did not significantly affect the amount of HCV RNA in the medium or cells (Fig. 3B and Supplemental Fig. 4B, black and white bars), whereas HCVcc in the medium was less infectious, as was observed when the cells treated with FR122047 (Fig. 3C and Supplemental Fig. 4C). Treatment with the TXAS inhibitor Ozagrel also dose-dependently suppressed infectious HCVcc production without significantly affecting HCV RNA levels in the medium or cells (Fig. 3D, E). Similar effects of Ozagrel were observed in another HCV cell culture system using Huh-7.5 cells and chimeric recombinant J6/JFH1 HCV, which encoded different structural proteins from JFH1[9] (Supplemental Fig. 5), indicating that our results were not specific to the JFH1 cell culture system. Furthermore, the treatment with PGH_2, a product of COX1 and a substrate of TXAS, showed to increase the infectivity of HCVcc without effect on the HCV replication and egression despite short half-life of PGH_2 (Supplemental Fig. 6). These data suggested that the AAC, in particular TXAS activity and probably TXA_2 produced from PGH_2 by TXAS activity, contributes to infectious HCV production.

TXA_2 receptor (TP) is not required for TXAS-dependent regulation of infectious HCV production

TXA_2 exerts its physiologic functions through TP on plasma membranes[17]. To examine the contribution of TXA_2/TP signaling, we investigated the effects of

the TP agonist U-46619 in our system. Regardless of dose, however, U-46619 did not affect infectious HCVcc production in the culture system (Supplemental Fig. 7A, B). Treating Huh-7–derived cell lines with the TP agonist did not increase the calcium ion concentration—a major downstream effect of TXA_2/TP signaling—even though the activity of U-46619 was confirmed in HEK293 cells[17] (Supplemental Fig. 8A). We also evaluated the activity of U-46619 in terms of TP dependent-activation of Rho and observed the Rho-dependent stress fiber formation induced with U-46619 in HEK293 cells (Supplemental Fig. 8B). In addition, the level of TP mRNA was, if any, quite low in human hepatocyte derived cells and PHH, although the only a small amount of the mRNA was detected in HuS-E/2 cells (Supplemental Fig. 3B). These data suggested that TXA_2/TP signal transduction is deficient in Huh-7–derived cell lines.

To determine whether TP on the Huh-7 cells was saturated with endogenous TXA_2 ligand, we examined the effects of U-46619 in the presence of Ozagrel. U-46619, however, did not rescue the Ozagrel-mediated suppression of infectious HCVcc production (Fig. 4A, B). Additionally, the TP antagonist daltroban did not affect infectious HCVcc production (Fig. 4C, D). These data indicated that TP-mediated signaling is not involved in TXAS-dependent regulation of infectious HCVcc production. Additionally, we examined whether thromboxane B_2 (TXB_2)—a stable metabolite of TXA_2 that does not activate TP—could be used to replace TXAS during infectious HCVcc production. TXB_2 did not counteract the effects of Ozagrel (Fig. 4A, B), and did not by itself affect the HCV lifecycle

(Supplemental Fig. 7A, B). These data suggested that TXA_2 or an unidentified metabolite of TXA_2 acts as a TP-independent regulator of infectious HCV production (see Discussion).

TXAS-derived signaling contributes to HCV infectivity

A previous study revealed that infectious HCV is produced near LDs to which HCV proteins are recruited[6]. As shown in Fig. 5A, inhibiting TXAS did not markedly affect the locations of the viral proteins Core and NS5A around LDs, suggesting that TXAS-derived signaling does not contribute to the recruitment of HCV proteins to the LDs. Next, to examine whether TXAS-mediated signaling drives the egression of infectious HCVcc from the cells, we analyzed intracellular HCVcc in cells treated with Ozagrel. Levels of intracellular HCVcc RNA in Huh-7 cells treated with or without Ozagrel were equivalent (Fig. 5B). Nevertheless, the infectivity of intracellular HCVcc from the cells treated with Ozagrel was markedly decreased as was that of HCVcc in the medium (Fig. 5C). This result indicated that TXAS-derived signaling is not involved in the release of infectious HCV particles. Taken together, it seemed likely that TXAS-derived signaling plays a role on infectious particle formation in the cells.

Inhibition of TXAS changes the physicochemical properties of HCVcc

We next analyzed HCVcc produced from cells treated with Ozagrel using sucrose density gradient ultracentrifugation. As reported previously[11], two types of fractions containing either highly infectious, low-density HCVcc (peak fraction

no. 6) or less infectious, high-density HCVcc (peak fraction no. 5) were obtained using samples derived from cells without treatment with Ozagrel, indicating that infectious HCVcc was mainly present in fraction no. 6 (Fig. 6, white bars, upper and lower panels). On the other hand, analyzing Ozagrel-treated cells revealed decreased levels of HCV RNA in fraction no. 6 (Fig. 6, solid lines, upper and lower panels). Of note, the amount of HCV RNA in fraction no. 5 remained similar with or without Ozagrel treatment (Fig. 6, lower panel). These results suggested that inhibition of TXAS-mediated signaling changed the physicochemical characteristics of HCVcc, resulting in altered infectivity.

A TXAS inhibitor and IP agonists inhibit early HCV expansion in bbHCV-infected chimeric mice

Finally, we examined the *in vivo* anti-HCV effects of a TXAS inhibitor using bbHCV and uPA/SCID mice bearing transplanted human hepatocytes. The IP agonist Beraprost was also tested, because PGI_2 produces effects opposite to TXA_2 during several physiologic processes, including vascular constriction in humans[25]. Both drugs delayed the increase in serum levels of HCV RNA (Fig. 7). Of note, even 4 weeks after treatment, Beraprost reduced serum HCV RNA levels to less than a quarter of those observed in control mice (Fig. 7). Our results indicated that these drugs may inhibit HCV proliferation *in vivo*, and that inhibition of TXAS-derived signaling and activation of IP-mediated PGI_2 signaling can control HCV proliferation. Although we examined the effects of the PGIS and IP agonist on the HCV lifecycle using the HCVcc-producing cell

culture system, Beraprost did not result in any notable changes (Supplemental Fig. 9). To examine whether the Huh-7 cells respond to the IP agonist, we assessed cAMP signaling using a plasmid bearing cAMP responsive elements in a promoter upstream of the luciferase gene; cAMP signaling is a major intracellular signaling pathway that is activated by IP agonists. The IP agonist, however, did not activate cAMP signaling in Huh-7 cells even though the pathway was activated in HuS-E/2 cells.

As another candidate anti-HCV drug, we examined the effect of ONO1301, possessing both TXAS inhibitor and IP agonist activities, in the humanized chimeric mice. ONO1301 produced the most robust suppression of HCV infections (Fig. 7). The effects of ONO1301 were also studied in the HCVcc-producing cell cultures; like Ozagrel. ONO1301 suppressed infectious HCV production (Supplemental Fig. 10), although ONO1301 did not activated cAMP signaling in Huh-7 cells (Supplemental Fig. 11). Slight decrease of HCVcc egression, however, caused by the treatment with ONO1301 at high concentrations might be of note. These results further supported our conclusion that TXAS-mediated signaling contributes to infectious HCV production, although the functional role of PGI_2 in this process is still unknown.

Discussion

In this study, we showed that TXAS is involved in the development of infectious HCV. Administration of a TXAS inhibitor inhibited early stages of HCV proliferation post-infection in a chimeric mouse model. These results suggest that TXAS-mediated infectious HCV production is a potential target for novel anti-HCV therapies.

We first found that inhibiting COX1 and TXAS decreased the infectivity of HCVcc in the culture medium without any significant effects on viral genome replication and particle egression (Fig. 2 and 3). In addition, we showed that inhibition of TXAS did not affect the release of infectious HCVcc from the cells (Fig. 5). Thus, we concluded that TXAS probably regulates HCV particle maturation and the development of infectivity. Knockdown of apolipoprotein E, heat shock protein 70, and annexin A2 expression was previously shown to inhibit infectious HCVcc production[26]. Of note, decreased expression of these host factors reduced the production of HCVcc in the culture medium as well as intracellular HCVcc levels in HCVcc-producing cells, suggesting that TXAS is playing a different role in HCVcc production. Moreover, our results suggest that TXAS is the first host factor that has been shown to contribute only to the development of HCV infectivity.

A previous study reported that infectious HCVcc is produced near LDs[11]. The HCV proteins Core and NS5A are located on and nearby LDs, respectively, suggesting a role in the production of infectious HCVcc[11]. Because LD localization of these proteins was not affected by the TXAS inhibitor (Fig. 5A), TXAS is probably required after these viral proteins are recruited to LDs.

Several studies have shown that the buoyant density of infectious HCVcc differs slightly from that of noninfectious HCVcc[11, 27, 28]. Infectious and noninfectious HCVcc are found in lower and higher density fractions, respectively. In the present study, inhibition of TXAS reduced the amount of HCVcc in the lower density fraction (fraction 6) containing the infectious particles, whereas levels of primarily noninfectious HCVcc particles in the higher density fraction (fraction 5) were not affected (Fig. 6). These results mirrored previously reported data about NS5A mutant HCVcc, which do not produce infectious particles[11]. These results suggested that TXAS might be required to produce infectious HCVcc near the LDs.

Studies with treatments with methyl-β-cyclodextrin or lipoprotein lipase have shown that changing the physicochemical properties of HCVcc[29, 3028, 29], in which the peak density fraction containing HCVcc shifted higher, diminished the infectivity of the particles[29, 30]. As TXAS inhibitors did not show the apparent shift to a higher density (Fig. 6), future molecular analyses of HCVcc particles should be required to reveal the underlying structural mechanisms for HCV infectivity.

Prostanoids play various physiologic functions, including regulatory roles in muscle and blood vessels[17]. Although inhibition of TXAS decreased the infectivity of HCVcc (Fig. 3), the identity of the relevant prostanoid and how that product functions in the development of infectious HCV are currently unclear. As the treatment of PGH_2, a substrate of TXAS, caused the increase of infectious HCV production (Supplemental Fig. 6), it seemed to be ruled out the possibility that supposedly accumulated PGH_2 by the treatment of TXAS inhibitor play a role in the inhibition. Although we analyzed the total fatty acids in

the HCV infected Huh-7.5 cells treated with and without Ozagrel, the compositions of fatty acids, including arachidonic acid (C20:4ω-6), were not largely different to each other (Supplemental Fig. 12), suggesting, at least, that the effect of Ozagrel is not due to major change of fatty acid composition.

The activity of the TXAS product TXA_2 was not directly examined, because its half-life is quite short[31]. Usually, TXA_2 activity is measured using stable agonists and antagonists of TP. We showed, however, that TP-mediated signaling is not related to the processes examined in the current study (Fig.4) It seemed likely that TXA_2 itself or an unidentified metabolite of TXA_2 mediates the development of HCV infectivity in a TP-independent manner. PGI_2 and the PGD_2 metabolite 15d-PGJ_2 have been identified as ligands of PPAR δ and γ, respectively[32, 33]. Therefore, the TXAS product may act as a ligand of various nuclear receptors to regulate infectious HCV production. In the PHH and the liver of chimeric mice transplanted with human hepatocyte, the expression of human TP mRNA was not observed (Supplemental Fig. 3A and 13), although that was detected in human liver tissue, consisting of many types of cells (Supplemental Fig. 13). It may be true, therefore, that TP gene is not largely expressed in human hepatocytes in the liver as with Huh-7 cells. Taken together, it is probable that infectious HCV are produced in TP-independent manner in human liver infected with HCV. Further studies regarding the TP-independent roles of TXAS products in hepatocytes may be required to elucidate the mechanisms of infectious HCV formation.

Recently, various drugs targeting viral proteins have been developed, resulting in more HCV-specific therapeutic profiles than those of conventional drugs[34]. Monotherapy with

an HCV-specific drug, however, sometimes fails to clear the HCV infection because of rapidly emerging resistant variants[35]. We found that a TXAS inhibitor and IP agonists suppressed early-stage expansion of bbHCV post-infection of chimeric mice bearing human hepatocytes (Fig. 7). These results clearly indicate that the TXAS inhibitor and IP agonist are novel candidates for anti-HCV drugs. In this experiment, the effects of an IP agonist and the TXAS inhibitor were compared, because TXA_2 and IP agonists have opposite clinical effects[20]. This implies that the IP agonist may have suppressed the effects of TXAS in the bbHCV-infected transplanted human hepatocytes. Contrary to our expectations, however, neither siRNA-mediated knockdown of PGIS expression nor treatment with the IP agonist Beraprost affected HCV genome replication, particle egression, or HCVcc infectivity (Supplemental Fig. 9). The responsiveness of Huh-7 cells to the IP agonist was then examined by monitoring activation of cAMP signaling, a pathway that is normally activated downstream of IP. The results demonstrated that Huh-7 cells were deficient in signaling from IP to intracellular cAMP production (Supplemental Fig. 11). Although the therapeutic mechanism of action for the IP agonist in the chimeric mice has not been clarified yet, the IP agonist may signal through IP to counteract TXA_2 signaling and suppress the effects of endogenous TXAS products on the formation of infectious HCV. In this in vivo experiments, the effect of drugs waned over time, especially in the case of Ozagrel. We examined the infectivity and the sensitivity against treatment with Ozagrel of HCV from the mice with the first drug treatment by secondary infection experiment. The results showed that HCV proliferated in the secondarily infected chimeric mice irrespective of the treatment of Ozagrel

(Supplemental Fig. 14), suggesting that HCV proliferating in the chimeric mice with first treatment acquired the resistance against Ozagrel. We analyzed partial genomic sequences of the drug resistant HCVs by the direct sequencing method. We found that 68 base substitutions, ten of which was accompanied with amino acid substitution, were present in such HCV genomes, compared to those in the mice untreated with the drug (Supplemental Fig. 15). This indicated that HCV, of which genome included a large number of base substitutions, actually proliferated in the chimeric mouse treated with Ozagrel. Further study of such drug resistant HCV, for examples, the reverse genetics analysis using recombinant HCV system, will help to reveal the molecular mechanisms of medicinal effect of this drug and the infectious HCV production. Furthermore, these results might demonstrate the needs to find the optimum dose of TXAS inhibitor for the effective therapy and to use this drug as one of options with different action mechanism for the multi-drug therapy.

References

1. Wasley A, Alter MJ. Epidemiology of hepatitis C: geographic differences and temporal trends. Semin Liver Dis 2000;20:1-16.
2. Younossi Z, Kallman J, Kincaid J. The effects of HCV infection and management on health-related quality of life. Hepatology 2007;45:806-816.
3. Fried MW, Shiffman ML, Reddy KR, et al. Peginterferon alfa-2a plus ribavirin for chronic hepatitis C virus infection. N Engl J Med 2002;347:975-982.
4. Gao M, Nettles RE, Belema M, et al. Chemical genetics strategy identifies an HCV NS5A inhibitor with a potent clinical effect. Nature 2010;465:96-100.
5. Chayama K, Takahashi S, Toyota J, et al. Dual therapy with the nonstructural protein 5A inhibitor, daclatasvir, and the nonstructural protein 3 protease inhibitor, asunaprevir, in hepatitis C virus genotype 1b-infected null responders. Hepatology 2012;55:742-748.
6. Lin C, Kwong AD, Perni RB. Discovery and development of VX-950, a novel, covalent, and reversible inhibitor of hepatitis C virus NS3.4A serine protease. Infect Disord Drug Targets 2006;6:3-16.
7. Sarrazin C, Zeuzem S. Resistance to direct antiviral agents in patients with hepatitis C virus infection. Gastroenterology 2010;138:447-462.
8. **Wakita T, Pietschmann T,** Kato T, et al. Production of infectious hepatitis C virus in tissue culture from a cloned viral genome. Nat Med 2005;11:791-796.
9. Lindenbach BD, Evans MJ, Syder AJ, et al. Complete replication of hepatitis C virus in cell culture. Science 2005;309:623-626.
10. **Zhong J, Gastaminza P,** Cheng G, et al. Robust hepatitis C virus infection in vitro. Proc Natl Acad Sci U S A 2005;102:9294-9299.

11. Miyanari Y, Atsuzawa K, Usuda N, et al. The lipid droplet is an important organelle for hepatitis C virus production. Nat Cell Biol 2007;9:1089-1097.
12. Aly HH, Watashi K, Hijikata M, et al. Serum-derived hepatitis C virus infectivity in interferon regulatory factor-7-suppressed human primary hepatocytes. J Hepatol 2007;46:26-36.
13. Aly HH, Qi Y, Atsuzawa K, et al. Strain-dependent viral dynamics and virus-cell interactions in a novel in vitro system supporting the life cycle of blood-borne hepatitis C virus. Hepatology 2009;50:689-696.
14. Aly HH, Shimotohno K, Hijikata M. 3D cultured immortalized human hepatocytes useful to develop drugs for blood-borne HCV. Biochem Biophys Res Commun 2009;379:330-334.
15. Chockalingam K, Simeon RL, Rice CM, et al. A cell protection screen reveals potent inhibitors of multiple stages of the hepatitis C virus life cycle. Proc Natl Acad Sci U S A 2010;107:3764-3769.
16. Gastaminza P, Whitten-Bauer C, Chisari FV. Unbiased probing of the entire hepatitis C virus life cycle identifies clinical compounds that target multiple aspects of the infection. Proc Natl Acad Sci U S A 2010;107:291-296.
17. Bos CL, Richel DJ, Ritsema T, et al. Prostanoids and prostanoid receptors in signal transduction. Int J Biochem Cell Biol 2004;36:1187-1205.
18. Little P, Skouteris GG, Ord MG, et al. Serum from partially hepatectomized rats induces primary hepatocytes to enter S phase: a role for prostaglandins? J Cell Sci 1988;91 (Pt 4):549-553.

19. Rudnick DA, Perlmutter DH, Muglia LJ. Prostaglandins are required for CREB activation and cellular proliferation during liver regeneration. Proc Natl Acad Sci U S A 2001;98:8885-8890.
20. Waris G, Siddiqui A. Hepatitis C virus stimulates the expression of cyclooxygenase-2 via oxidative stress: role of prostaglandin E2 in RNA replication. J Virol 2005;79:9725-9734.
21. Tateno C, Yoshizane Y, Saito N, et al. Near completely humanized liver in mice shows human-type metabolic responses to drugs. Am J Pathol 2004;165:901-912.
22. Kushima Y, Wakita T, Hijikata M. A disulfide-bonded dimer of the core protein of hepatitis C virus is important for virus-like particle production. J Virol 2010;84:9118-9127.
23. Gastaminza P, Kapadia SB, Chisari FV. Differential biophysical properties of infectious intracellular and secreted hepatitis C virus particles. J Virol 2006;80:11074-11081.
24. Kamiya N, Iwao E, Hiraga N, et al. Practical evaluation of a mouse with chimeric human liver model for hepatitis C virus infection using an NS3-4A protease inhibitor. J Gen Virol 2010;91:1668-1677.
25. Flavahan NA. Balancing prostanoid activity in the human vascular system. Trends Pharmacol Sci 2007;28:106-110.
26. Bartenschlager R, Penin F, Lohmann V, et al. Assembly of infectious hepatitis C virus particles. Trends Microbiol 2011;19:95-103.

27. Andre P, Komurian-Pradel F, Deforges S, et al. Characterization of low- and very-low-density hepatitis C virus RNA-containing particles. J Virol 2002;76:6919-6928.
28. Nielsen SU, Bassendine MF, Burt AD, et al. Association between hepatitis C virus and very-low-density lipoprotein (VLDL)/LDL analyzed in iodixanol density gradients. J Virol 2006;80:2418-2428.
29. Aizaki H, Morikawa K, Fukasawa M, et al. Critical role of virion-associated cholesterol and sphingolipid in hepatitis C virus infection. J Virol 2008;82:5715-5724.
30. Shimizu Y, Hishiki T, Sugiyama K, et al. Lipoprotein lipase and hepatic triglyceride lipase reduce the infectivity of hepatitis C virus (HCV) through their catalytic activities on HCV-associated lipoproteins. Virology 2010;407:152-159.
31. Gryglewski RJ. Prostacyclin among prostanoids. Pharmacol Rep 2008;60:3-11.
32. Forman BM, Tontonoz P, Chen J, et al. 15-Deoxy-delta 12, 14-prostaglandin J2 is a ligand for the adipocyte determination factor PPAR gamma. Cell 1995;83:803-812.
33. Gupta RA, Tan J, Krause WF, et al. Prostacyclin-mediated activation of peroxisome proliferator-activated receptor delta in colorectal cancer. Proc Natl Acad Sci U S A 2000;97:13275-13280.
34. Pawlotsky JM, Chevaliez S, McHutchison JG. The hepatitis C virus life cycle as a target for new antiviral therapies. Gastroenterology 2007;132:1979-1998.
35. Wohnsland A, Hofmann WP, Sarrazin C. Viral determinants of resistance to treatment in patients with hepatitis C. Clin Microbiol Rev 2007;20:23-38.

1 Author names in bold designate shared co-first authorship.

Figure Legends.

Figure 1. PG synthase mRNA expression under 3D culture conditions. (A) Results of microarray analysis. Black and white bars represent mRNA expression levels in HuS-E/2 cells cultured with Mebiol gel and hollow fibers, respectively, relative to levels observed in cells cultured under 2D conditions. Gray bars represent mRNA expression levels in HuS-E/2 cells cultured with Mebiol gel by quantifying with quantitative RT-PCRs. qRT-PCR data shows that averages from quadruplicate samples in two independent experiments ± SD are shown. * differs from Control, $P < .01$; ** differs from Control, $P < .001$. (B) Protein levels of TXAS and various PG synthases in 2D-cultured and 3D-cultured HuS-E/2 cells. PG synthases except for TXAS were detected in whole cell lysate. Asterisks show the result in membrane fraction.

Figure 2. Effects of FR122047 on HCVcc-producing Huh-7 cells. (A) Effects of FR122047 on HCV RNA levels in cultured HCVcc-producing cells. HCV RNA was collected from the medium (black bars) and cells (white bars), which were treated with FR122047 at the indicated concentrations. Mean cell viability ± SD for each sample condition is also plotted (gray bars). Averages from quadruplicate samples in two independent experiments ± SD are shown. (B) Effects of FR122047 on the infectivity of HCVcc produced using this cell culture system. (C) FR122047 reduces infectious HCVcc in the culture medium. Huh-7.5 cells infected with HCVcc from the culture medium of cells treated with (right panel) and without (left panel) FR122047 at the indicated concentrations were stained with anti-HCV antibodies (magenta) and the

nuclear stain 4',6-diamidino-2-phenylindole (DAPI; cyan). Lower panels show infected cells at lower titer of inoculums. * differs from Control, $P < .01$; ** differs from Control, $P < .001$.

Figure 3. Effect of TXAS on infectious HCV production. (A) siRNA-mediated knockdown of TXAS mRNA expression. (B) Effects of TXAS-specific siRNA on HCV RNA levels in the HCVcc-producing cell culture system. (C) Effects of control and TXAS-specific siRNA on the infectivity of HCVcc in medium obtained from HCVcc-producing cell cultures were assessed. (D) Effects of Ozagrel on HCV RNA levels were assessed in HCVcc-producing cell cultures. (E) Effects of Ozagrel on the infectivity of HCVcc produced from the cell culture system were assessed. * differs from Control, $P < .01$; ** differs from Control, $P < .001$.

Figure 4. Role of TP in infectious HCVcc-producing cell cultures. (A) Effects of U-46619 and TXB_2 on HCV RNA levels in HCVcc-producing cell cultures in the presence of Ozagrel were assessed. (B) The infectivity of HCVcc in culture medium from HCVcc-producing cells treated with U-46619 or TXB_2 in the presence of Ozagrel was assessed. (C) Effect of daltroban on HCV RNA levels in HCVcc-producing cell cultures. (D) The infectivity of HCVcc in culture medium from HCVcc-producing cells treated with daltroban. * differs from Control, $P < .01$; ** differs from Control, $P < .001$.

Figure 5. Core and NS5A near LDs and the quantity and infectivity of intracellular HCVcc. (A) HCV Core (magenta) and NS5A (cyan) around LDs (yellow) in HCVcc-producing cells treated with the indicated reagents were observed using immunofluorescence analysis. Nuclei were stained with DAPI (gray). Scale bars, 5 μm. (B) Levels of intracellular HCV RNA obtained from the cells treated with Ozagrel. (C) The infectivity of intracellular HCV from cells treated with Ozagrel. Averages of triplicate samples from two independent experiments ± SD are shown. ** differs from Control, $P < .001$.

Figure 6. Buoyant density of HCVcc produced from cells treated with Ozagrel. Lower and upper panels show the results of HCVcc from the cells with and without Ozagrel treatment, respectively. HCV RNA (solid line), fraction density (dotted line) and HCV infectivity (white bars) in each fraction collected after ultracentrifugation are shown. Representative results from two independent experiments are shown.

Figure 7. Effects of ONO1301, Beraprost, Ozagrel, and Telaprevir on the expansion of bbHCV-infected uPA/SCID mice bearing human hepatocytes. Data are presented as means ± SD for six (control, diamonds), four (ONO1301, squares; Ozagrel, crosses; Telaprevir, asterisk), and three (Beraprost, triangles) samples. * differs from Control, $P < .05$.

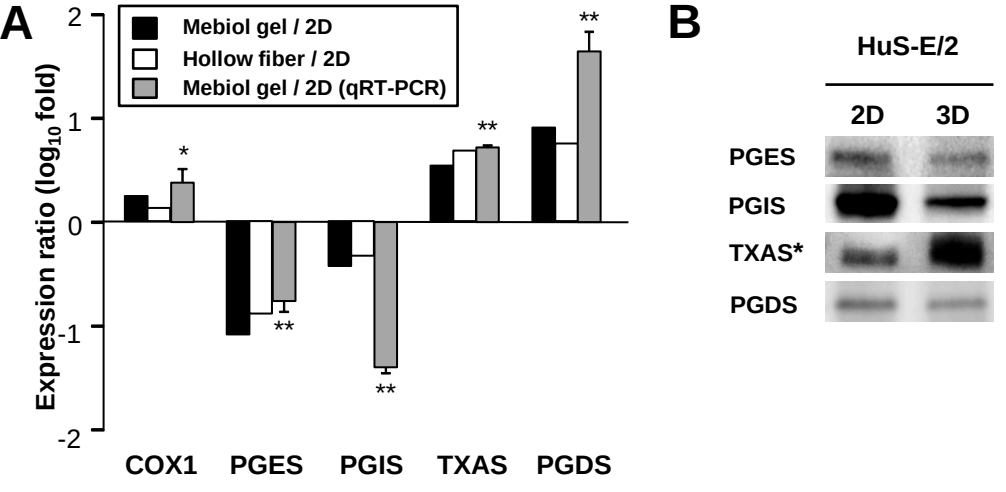
A
Mebiol gel / 2D
Hollow fiber / 2D
Mebiol gel / 2D (qRT-PCR)
Expression ratio (log10 fold)
2
1
0
-1
-2
*
**
**
**
**
COX1
PGES
PGIS
TXAS
PGDS
B
HuS-E/2
2D
3D
PGES
PGIS
TXAS*
PGDS

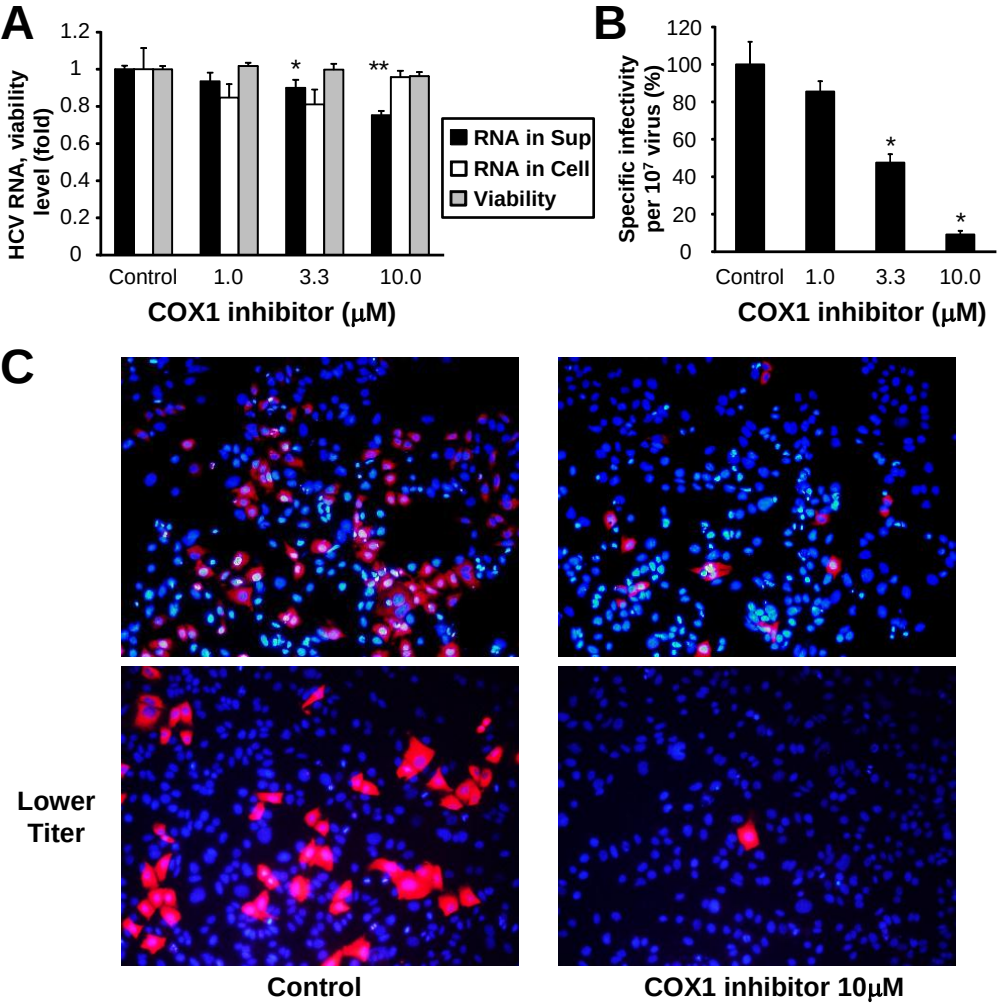
A
HCV RNA, viability level (fold)
1.2
1
0.8
0.6
0.4
0.2
0
*
**
RNA in Sup
RNA in Cell
Viability
Control
1.0
3.3
10.0
COX1 inhibitor (μM)
B
Specific infectivity per 10^7 virus (%)
120
100
80
60
40
20
0
*
*
Control
1.0
3.3
10.0
COX1 inhibitor (μM)
C
Lower Titer
Control
COX1 inhibitor 10μM

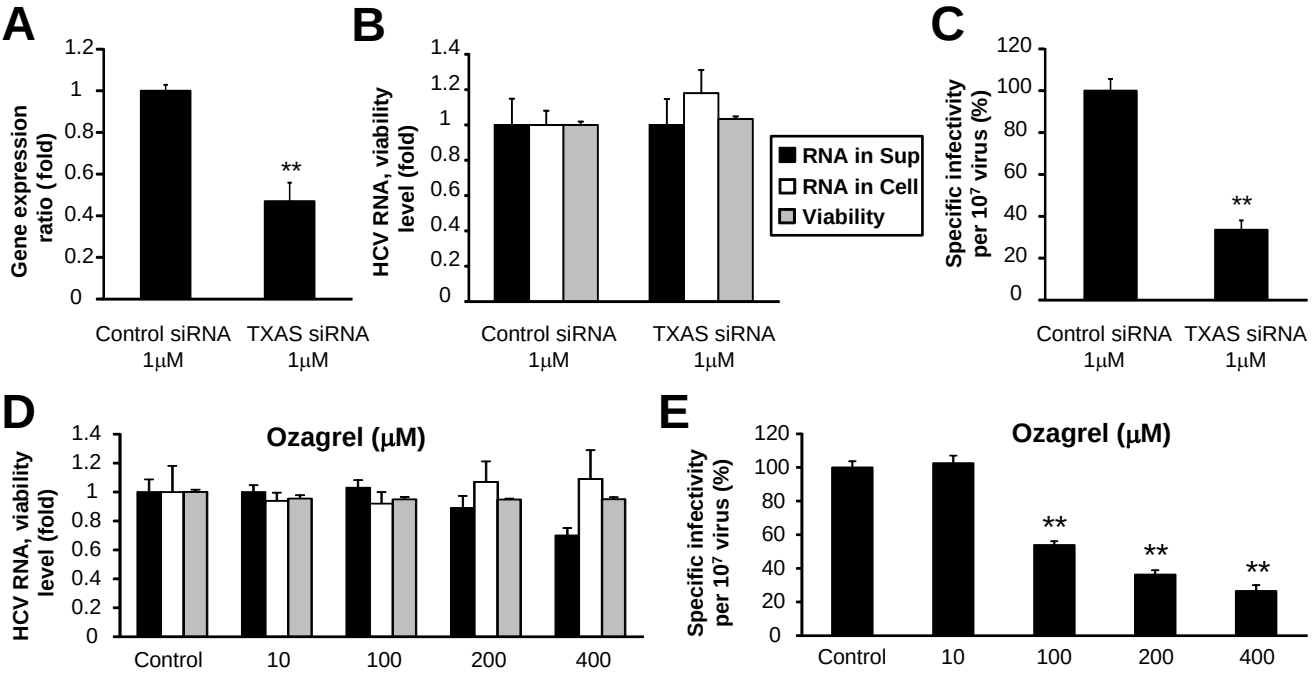
A
Gene expression ratio (fold)
1.2
1
0.8
0.6
0.4
0.2
0
**
Control siRNA 1μM
TXAS siRNA 1μM
B
HCV RNA, viability level (fold)
1.4
1.2
1
0.8
0.6
0.4
0.2
0
RNA in Sup
RNA in Cell
Viability
Control siRNA 1μM
TXAS siRNA 1μM
C
Specific infectivity per 10⁷ virus (%)
120
100
80
60
40
20
0
**
Control siRNA 1μM
TXAS siRNA 1μM
D
Ozagrel (μM)
HCV RNA, viability level (fold)
1.4
1.2
1
0.8
0.6
0.4
0.2
0
Control
10
100
200
400
E
Ozagrel (μM)
Specific infectivity per 10⁷ virus (%)
120
100
80
60
40
20
0
**
**
**
Control
10
100
200
400

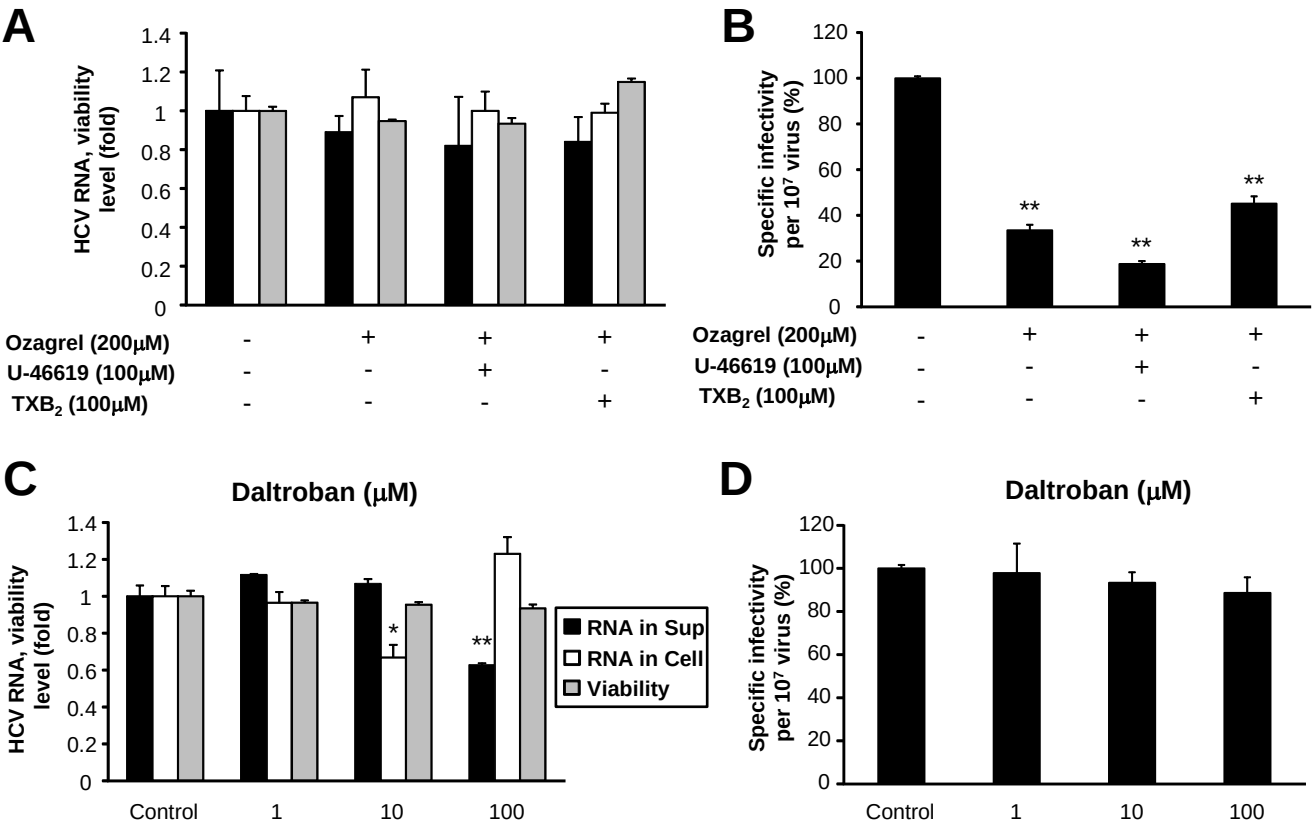
A
HCV RNA, viability level (fold)
1.4
1.2
1
0.8
0.6
0.4
0.2
0
Ozagrel (200μM) - + + +
U-46619 (100μM) - - + -
TXB2 (100μM) - - - +
B
Specific infectivity per 10^7 virus (%)
120
100
80
60
40
20
0
**
**
**
Ozagrel (200μM) - + + +
U-46619 (100μM) - - + -
TXB2 (100μM) - - - +
C
Daltroban (μM)
HCV RNA, viability level (fold)
1.4
1.2
1
0.8
0.6
0.4
0.2
0
*
**
RNA in Sup
RNA in Cell
Viability
Control
1
10
100
D
Daltroban (μM)
Specific infectivity per 10^7 virus (%)
120
100
80
60
40
20
0
Control
1
10
100

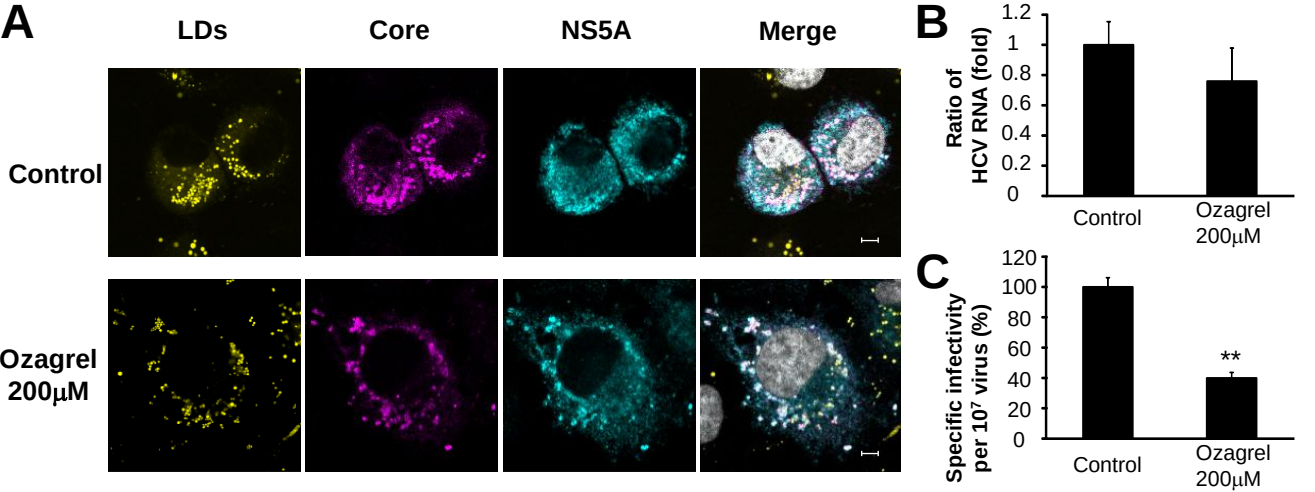
A
LDs
Core
NS5A
Merge
Control
Ozagrel
200μM
B
Ratio of
HCV RNA (fold)
1.2
1
0.8
0.6
0.4
0.2
0
Control
Ozagrel
200μM
C
Specific infectivity
per 10⁷ virus (%)
120
100
80
60
40
20
0
**
Control
Ozagrel
200μM

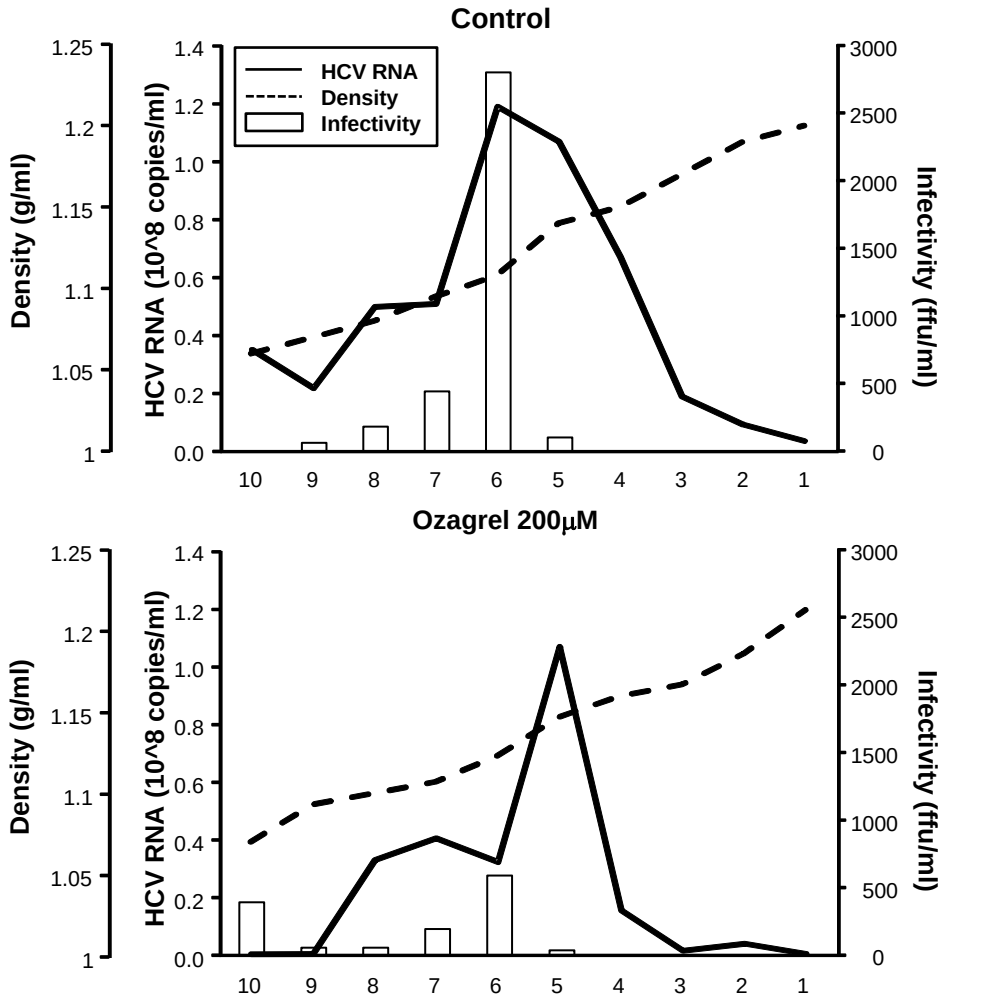
Control
HCV RNA
Density
Infectivity
Density (g/ml)
HCV RNA (10^8 copies/ml)
Infectivity (ffu/ml)
1.25
1.2
1.15
1.1
1.05
1
1.4
1.2
1.0
0.8
0.6
0.4
0.2
0.0
3000
2500
2000
1500
1000
500
0
10 9 8 7 6 5 4 3 2 1
Ozagrel 200μM
Density (g/ml)
HCV RNA (10^8 copies/ml)
Infectivity (ffu/ml)
1.25
1.2
1.15
1.1
1.05
1
1.4
1.2
1.0
0.8
0.6
0.4
0.2
0.0
3000
2500
2000
1500
1000
500
0
10 9 8 7 6 5 4 3 2 1

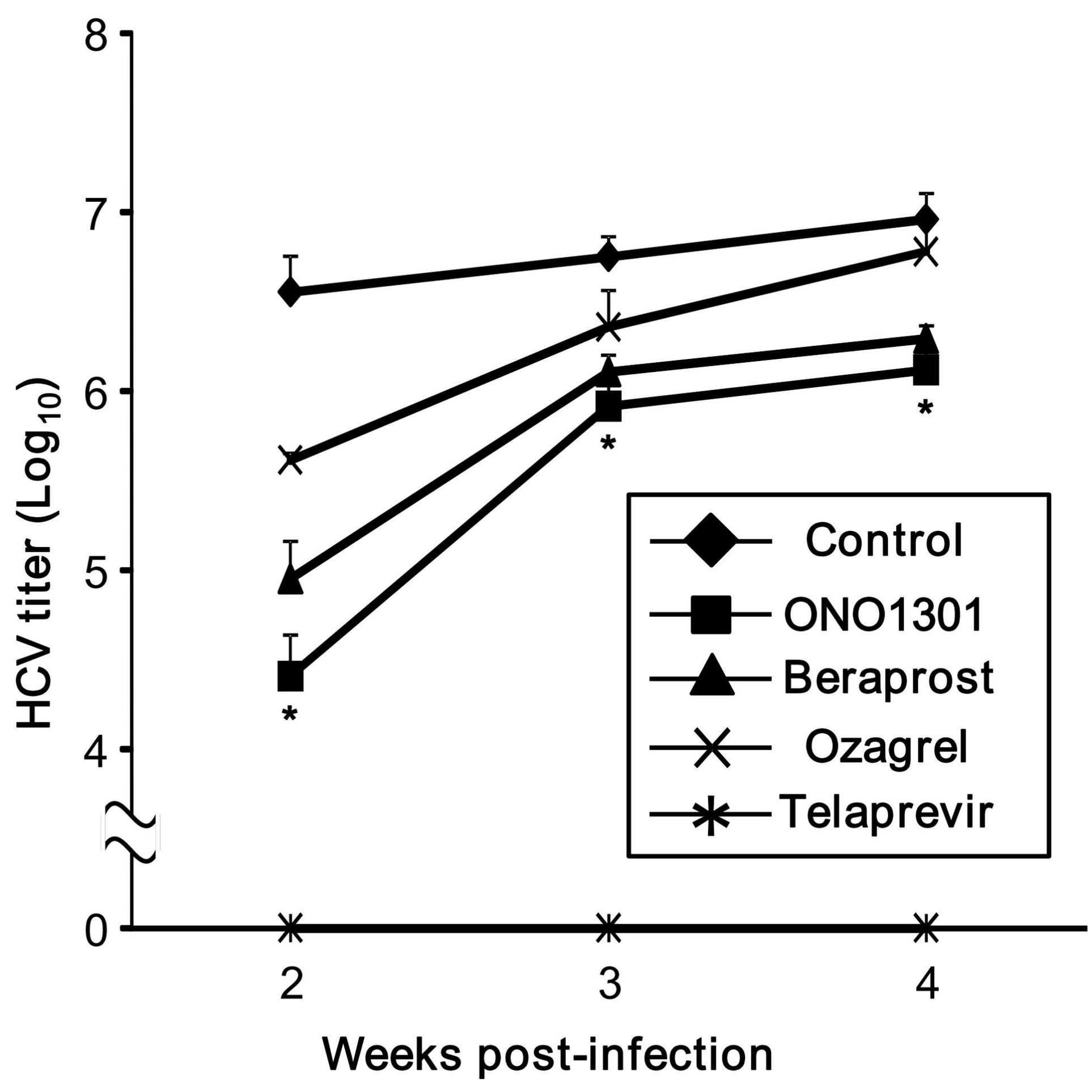
8
7
6
5
4
0
HCV titer (Log10)
2
3
4
Weeks post-infection
*
*
*
Control
ONO1301
Beraprost
Ozagrel
Telaprevir

Supplemental Materials and Methods

Preparation of subcellular fraction and protein detection with western blotting

Subcellular fractions of HuS-E/2 cells and patient's tissues were prepared by use of ProteoExtract Subcellular proteome Extraction Kit (Millipore, Massachusetts, USA) according to manufacturer's protocol. Five μg of total protein of each fraction or whole cell lysate of each cells was analyze by western blotting. Western blotting was performed as described previously[1].

Collection of total RNA and cell lysate from HCV-infected patients' tissue

Total RNA from patients' tissue was collected with RNeasy mini (Qiagen, Hilden, Germany). In briefly, frozen tissues were homogenized in lysis buffer with Power Masher (Nippi, Tokyo, Japan). Homogenized samples were used for RNA purification according to manufacturer's protocol. Cell lysate from tissues were collected with RIPA buffer (Thermo Scientific, Massachusetts, USA) or ProteoExtract Subcellular proteome Extraction Kit according to manufacturer's protocol.

cAMP reporter assay

Huh-7-derived and HuS-E/2 cells were transfected with pCRE-Luc (Agilent Technologies, California, USA) using Fugene6 (Roche) and Effectene (Qiagen, Hilden, Germany), respectively, essentially according to the manufacturers' protocols. Six hours and two days post-transfection of Huh-7–derived and HuS-E/2 cells, respectively, the culture medium was replaced with fresh medium containing one of the reagents. One and three day(s) post-transfection of Huh-7–derived and HuS-E/2 cells, respectively, luciferase activity in the cells was measured using a luciferase activity detection reagent (Promega, Wisconsin, USA) and Lumat LB 9507 luminometer (EG&G Berthold, Bad Wildbad, Germany).

Prostanoid signals as anti-HCV targets

Calcium ion quantification

HEK293, Huh-7-derived, and HuS-E/2 cells were treated with the calcium ionosphere A23187 (Sigma-Aldrich) and the TXA_2 receptor (TP) agonist U-46619 for 1 day. Calcium ion concentrations were quantified using a calcium assay kit (Cayman Chemical) according to the manufacturer's protocols.

Actin polymerization assay

An activation of actin polymerization via TP was measured with fluorescein isothiocyanate (FITC)-phalloidin (Sigma-Aldrich). After cultured in lipid-free fresh medium, cells were stimulated with 10 μM U46619 containing medium for 30, 60, and 180 sec. Then, samples were stained with 10 μg/ml FITC-phalloidin, Fluorescent intensity at 520 nm was measured.

Fatty acid analysis

Fatty acid analysis of HCV-infected Huh7.5 cells treated with or without Ozagrel was performed by Toray Research Center, INC. in Japan using gas chromatogray. Total fatty acids samples were extracted from the cells according to Bligh-Dyer method[2].

Secondary infection experiments in chimeric mice transplanted human hepatocyte

The chimeric mice were inoculated intravenously with patient serum including 1.0×10^5 genome titer of bbHCV (genotype 1b) as the first infection. Ozagrel was orally administrated twice each day (300 μg/day) one week after the inoculation. The serum samples from those mice were collected at 5 weeks after starting the drug treatments, and used as inocula in the secondary infection experiment. Naïve chimeric mice were

inoculated with the collected chimeric mice serum including 1.0 x 10^5 genome titer of HCV. Administration of Ozagrel was started simultaneously. HCV RNA levels in the blood of the chimeric mice at 1, 2 and 3 weeks post infection in secondary infection experiments were evaluated by quantitative RT-PCR.

Determination of nucleotide sequence of HCV genome after the treatment of Ozagrel

Chimeric mice were secondary inoculated with sera from HCV infected chimeric mice with or without the treatment of Ozagrel. Sera of these chimeric mice treated with or without Ozagrel were collected five weeks after the inoculation and the start of the treatment. HCV genome sequences of these samples were determined by the direct sequencing method according to the protocol described previously[3]. Obtained HCV genomic sequences from sera of mice with two different types of treatment were compared to each other. Mice with two different types of treatments were as follows; A. Mice inoculated secondarily with sera from 1st chimeric mouse without treatment were not treated with the drug (BankIt1626925 Seq3 in GenBank). B. Mice inoculated secondarily with sera from 1st chimeric mouse with treatment were treated with the drug (BankIt1626925 Seq1 in GenBank). These sequencing data were registered with GenBank (http://www.ncbi.nlm.nih.gov/genbank/).

Figure Legends

Supplemental Figure 1. Protein and mRNA levels of PG synthases in HCV-infected patient's tissue. (A), (B) mRNA expression and protein levels of PG synthases in HCV-infected patient's tissue. Representative results from two independent experiments are shown.

Supplemental Figure 2. Effects of COX2 inhibitor 1 on infectious HCV production. (A) Effects of COX2 inhibitor 1 on HCV RNA levels in the HCVcc-producing cell culture system. Levels of HCV RNA in medium (black bars) and cells (white bars) treated with or without COX2 inhibitor 1 were assessed with quantitative RT-PCRs and are plotted as amounts relative to results observed with control cells (control). Mean cell viability ± SD for each sample condition is also plotted (gray bars). (B) Effects of COX2 inhibitor 1 on the infectivity of HCVcc produced using the cell culture system. (C) Expression of COX2 mRNA in MH14 (positive control), Huh-7, and JFH1-transfected Huh-7 cells. * differs from Control, $P < .01$; ** differs from Control, $P < .001$.

Supplemental Figure 3. Expression of PG synthase and PG receptor mRNA in immortalized and primary hepatocyte cell lines. (A), (B) mRNA expression levels of various PG synthases and PG receptors in HuS-E/2 cells, Huh-7 cells, Huh-7.5 cells, and primary human hepatocytes were analyzed in RT-PCRs. Representative results from two independent experiments are shown.

Supplemental Figure 4. Effects of short hairpin RNA (shRNA)-mediated knockdown of TXAS mRNA levels on infectious HCV production. (A) Knockdown of TXAS mRNA levels using shRNA. (B) Effects of TXAS-specific shRNA on HCV RNA levels in the HCVcc-producing cell culture system. Levels of HCV RNA in medium (black bars) and

cells (white bars) treated with control or TXAS-specific shRNA were assessed with quantitative RT-PCRs and are plotted as amounts relative to results observed with control shRNA–treated cells (control). Mean cell viability ± SD for each sample condition is also plotted (gray bars). (C) Effects of TXAS-specific shRNA on the infectivity of HCVcc produced using the cell culture system. ** differs from Control, $P < .001$.

Supplemental Figure 5. Effects of Ozagrel and ONO1301 on the infectivity of HCVcc produced from J6/JFH1-transfected Huh-7.5 cells. (A) Effects of Ozagrel (upper panel) and ONO1301 (lower panel) on HCV RNA levels in HCVcc-producing cell cultures. Levels of HCV RNA in the medium (black bars) and cells (white bars) treated with Ozagrel or ONO1301 cells were assessed in quantitative RT-PCRs and are plotted as the amount relative to results from untreated cells (control). Mean cell viability ± SD for each sample condition is also plotted (gray bars). (B) Effects of Ozagrel (upper panel) and ONO1301 (lower panel) on the infectivity of HCVcc produced in the cell culture system. * differs from Control, $P < .01$; ** differs from Control, $P < .001$.

Supplemental Figure 6. Effects of PGH_2 on infectious HCV production. (A) Effects of PGH_2 on HCV RNA levels in the HCVcc-producing cell culture system. Levels of HCV RNA in medium (black bars) and cells (white bars) treated with or without PGH_2 were assessed with quantitative RT-PCRs and are plotted as amounts relative to results observed with control cells (control). Mean cell viability ± SD for each sample condition is also plotted (gray bars). (B) Effects of PGH_2 on the infectivity of HCVcc produced using the cell culture system. * differs from Control, $P < .01$; ** differs from Control, $P < .001$.

Supplemental Figure 7. Effects of U-46619 and TXB_2 on infectious HCV production. (A) Effects of U-46619 (upper panel) and TXB_2 (lower panel) on HCV RNA levels in HCVcc-producing cell cultures. Levels of HCV RNA in the medium (black bars) and cells (white bars) treated with U-46619 or TXB_2 were assessed in quantitative RT-PCRs and are plotted as the amount relative to results observed with untreated cells (control). Mean cell viability ± SD for each sample condition is also plotted (gray bars). (B) Effects of U-46619 (upper panel) and TXB_2 (lower panel) on the infectivity of HCVcc produced in the cell culture system were assessed.

Supplemental Figure 8. Effects of U-46619 on HuS-E/2, Huh-7, Huh-7.5, and HEK293 cell lines via TP. (A) Concentrations of intracellular calcium ions were measured in HuS-E/2 (black bars), Huh-7 (white bars), Huh-7.5 (gray bars), and HEK293 (dark gray bars) cells treated with or without a calcium ionophore or U-46619. Calcium ion concentrations relative to those in mock treated cells (control) were determined from triplicate wells in two independent experiments and are shown as means ± SD. (B) Actin polymerization after U-46619 treatment was measured with FITC-labeled phalloidin. * differs from Control, $P < .01$; ** differs from Control, $P < .001$

Supplemental Figure 9. Effects of PGI_2 on infectious HCV production. (A) siRNA-mediated knockdown of PGIS expression. (B) Effects of PGIS-specific siRNA on HCV RNA levels in HCVcc-producing cell cultures. Levels of HCV RNA in medium (black bars) and cells (white bars) treated with control or PGIS-specific siRNA were assessed in quantitative RT-PCR and are plotted as amounts relative to results obtained with control siRNA–treated cells (control). Mean cell viability ± SD for each sample condition is also plotted (gray bars). (C) Effects of PGIS-specific siRNA on the infectivity of HCVcc produced in the cell culture system. (D) Effects of Beraprost on HCV RNA levels in

HCVcc-producing cell cultures. Levels of HCV RNA in medium (black bars) and HCVcc-producing Huh-7 cells (white bars) treated with Beraprost were assessed in quantitative RT-PCRs and are plotted as amounts relative to results obtained with untreated cells (control). Mean cell viability ± SD for each sample condition is also plotted (gray bars). (E) Effects of Beraprost on the infectivity of HCVcc in culture medium from HCVcc-producing cell cultures were assessed. * differs from Control, $P < .01$

Supplemental Figure 10. Effects of ONO1301 on HCV lifecycle. (A) Levels of HCV RNA in medium (black bars) and cells (white bars) treated with or without ONO1301 were assessed. Mean cell viability ± SD for each sample condition is also plotted (gray bars). (B) The infectivity of HCVcc in culture medium from HCVcc-producing cell cultures treated with or without ONO1301 was assessed. (C) Subcellular locations of HCV Core and NS5A proteins around LDs in the presence of ONO1301. Scale bars, 5 μm. (D), (E) Levels and infectivity of intracellular HCV obtained from the cells treated with ONO1301. (F) Buoyant density of HCVcc obtained using cells treated with ONO1301. The panel shows HCV RNA (solid line), fraction density (dotted line) and HCV infectivity (white bars) in each fraction collected by ultracentrifugation. * differs from Control, $P < .01$; ** differs from Control, $P < .001$.

Supplemental Figure 11. Effects of dibutyryl cAMP (dbcAMP) on cell cultures producing JFH1 HCVcc. (A) HuS-E/2 (black bars), Huh-7 (white bars), and Huh-7.5 (gray bars) cells were transfected with CRE-Luc plasmid. Then, the luciferase activity in each sample was measured. Values were obtained from quadruplicate wells in two independent experiments and are shown as means ± SD. (B) Effects of dbcAMP on HCV RNA levels in HCVcc-producing cell cultures. Levels of HCV RNA in medium (black bars) and cells treated with dbcAMP (white bars) were assessed in quantitative

RT-PCRs and are plotted as amounts relative to results obtained with mock-treated cells (control). Mean cell viability ± SD for each sample condition is also plotted (gray bars). (C) Effects of dbcAMP on the infectivity of HCVcc produced using the cell culture system. * differs from Control, $P < .01$; ** differs from Control, $P < .001$.

Supplemental Figure 12. Comparison of composition of fatty acids in HCV-infected Huh7.5 cells with or without the treatment of Ozagrel.

Supplemental Figure 13. Expression of TP mRNA in liver tissues from Human patients and chimeric mice infected with HCV.

Supplemental Figure 14. Secondary infection of HCV derived from chimeric mice model. Data are presented as means ± SD for four samples.

Supplemental Figure 15. Base substitutions in HCV genome collected from mice serum during secondary infection. HCV genomic sequences from mice sera with the treatment of Ozagrel during primary and secondary infection was compared to those from mice without any treatment during both infection experiments. The region of obtained HCV genomic sequences is indicated by a thick bar. The nucleotide positions of each base substitution are shown with arrows. Positions of base substitutions, and types of base substitution and amino acid replacement are listed at lower panel.

Tables

Supplemental Table 1. Primer sequences and parameters in RT-PCR experiments. RT-PCRs were performed as follows: 25–40 cycles of 95°C for 30 seconds, 55–62°C for 30 seconds, and 72°C for 1 minute.

Supplemental Table 2. Primer sequences and parameters in qRT-PCR experiments. qRT-PCRs were performed as follows: 40 cycles of 95°C for 5 seconds, 60°C for 34 seconds.

Supplemental Reference

1. Kushima Y, Wakita T, Hijikata M. A disulfide-bonded dimer of the core protein of hepatitis C virus is important for virus-like particle production. J Virol 2010;84:9118-9127.
2. Bligh EG, Dyer WJ. A rapid method of total lipid extraction and purification. Can J Biochem Physiol 1959;37:911-917.
3. Kimura T, Imamura M, Hiraga N, et al. Establishment of an infectious genotype 1b hepatitis C virus clone in human hepatocyte chimeric mice. J Gen Virol 2008;89:2108-2113.

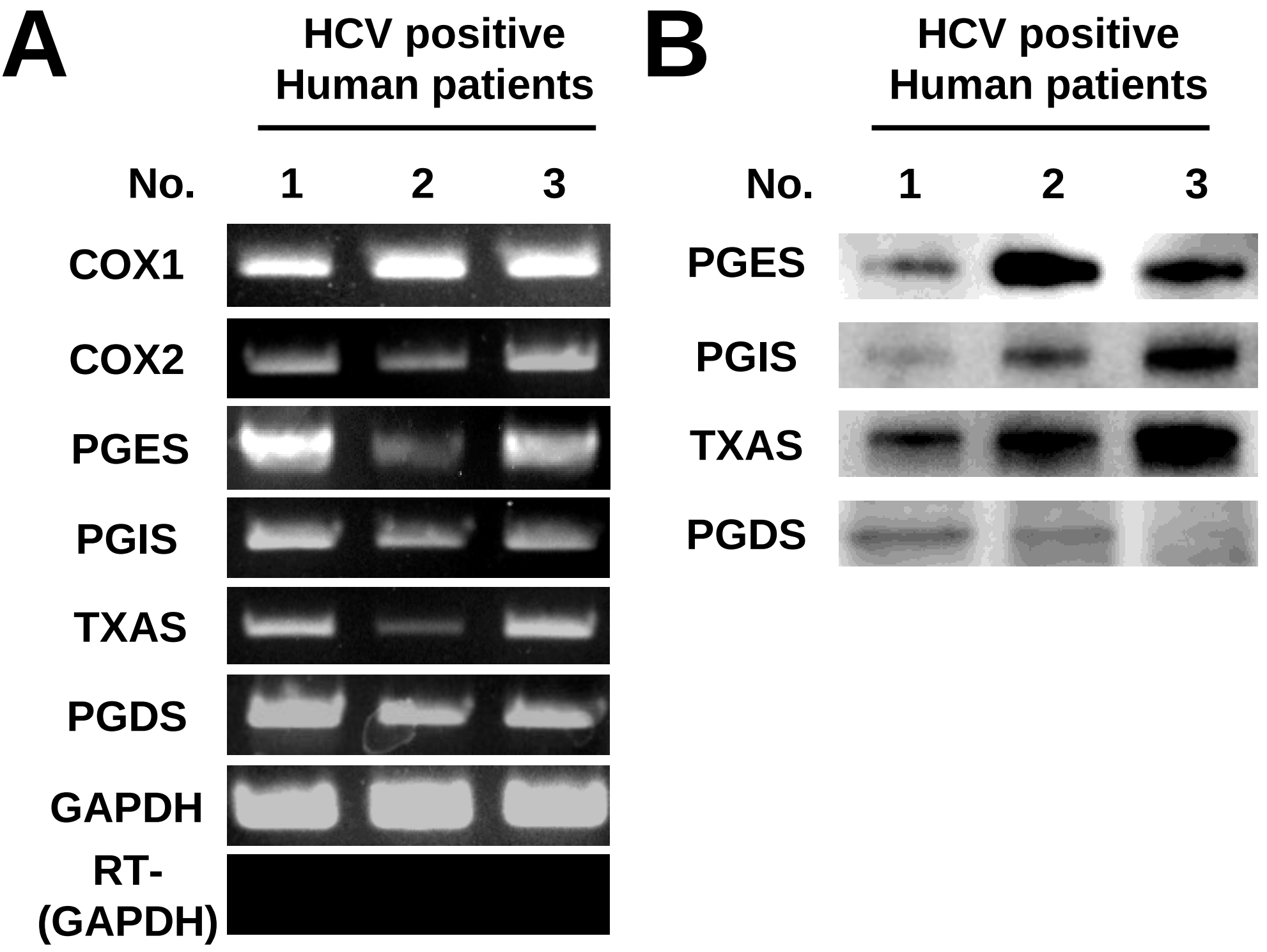
A
HCV positive
Human patients
No.
1
2
3
COX1
COX2
PGES
PGIS
TXAS
PGDS
GAPDH
RT-
(GAPDH)
B
HCV positive
Human patients
No.
1
2
3
PGES
PGIS
TXAS
PGDS

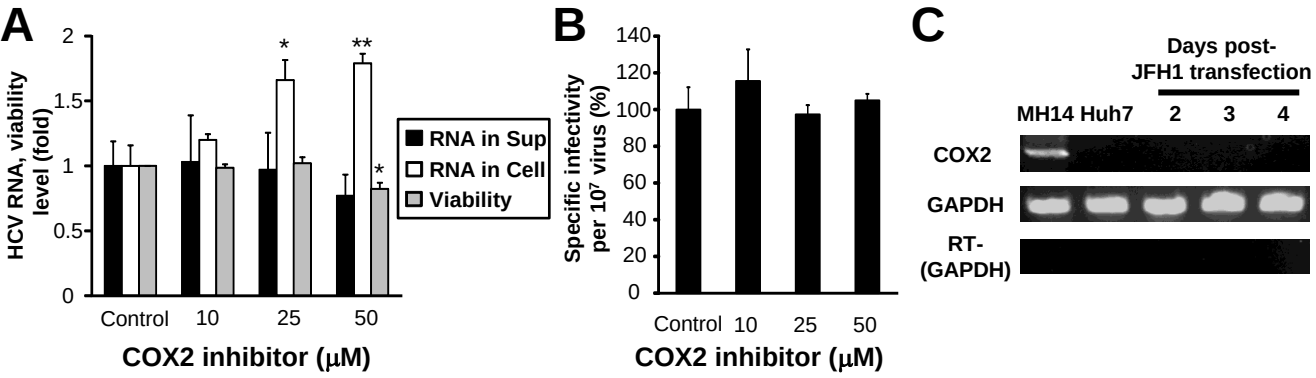
A
HCV RNA, viability level (fold)
2
1.5
1
0.5
0
*
**
*
RNA in Sup
RNA in Cell
Viability
Control
10
25
50
COX2 inhibitor (μM)
B
Specific infectivity per 10⁷ virus (%)
140
120
100
80
60
40
20
0
Control
10
25
50
COX2 inhibitor (μM)
C
Days post-JFH1 transfection
MH14
Huh7
2
3
4
COX2
GAPDH
RT-(GAPDH)

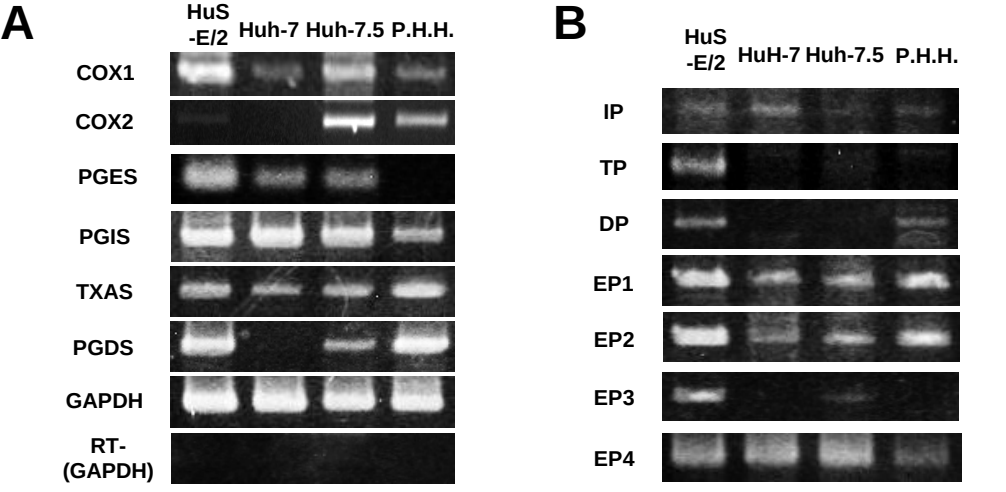
A
HuS -E/2
Huh-7
Huh-7.5
P.H.H.
COX1
COX2
PGES
PGIS
TXAS
PGDS
GAPDH
RT- (GAPDH)
B
HuS -E/2
HuH-7
Huh-7.5
P.H.H.
IP
TP
DP
EP1
EP2
EP3
EP4

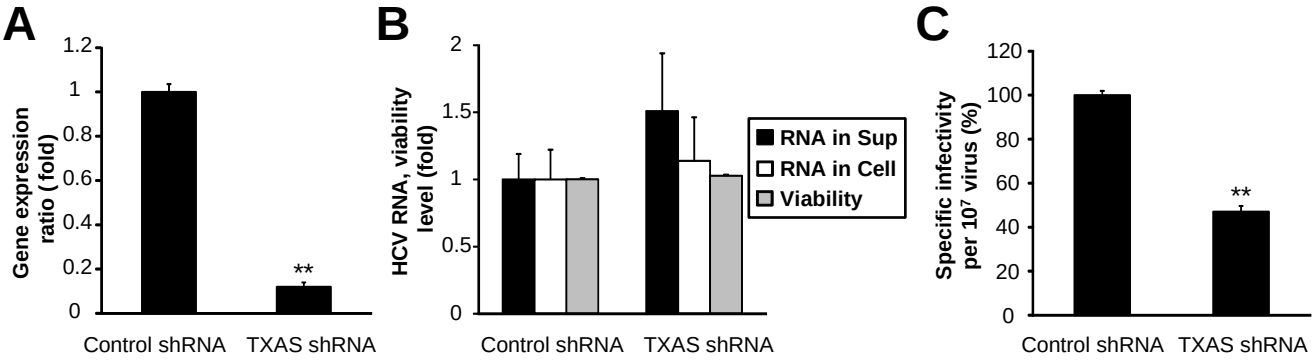
A
Gene expression ratio (fold)
1.2
1
0.8
0.6
0.4
0.2
0
**
Control shRNA
TXAS shRNA
B
HCV RNA, viability level (fold)
2
1.5
1
0.5
0
RNA in Sup
RNA in Cell
Viability
Control shRNA
TXAS shRNA
C
Specific infectivity per 10^7 virus (%)
120
100
80
60
40
20
0
**
Control shRNA
TXAS shRNA

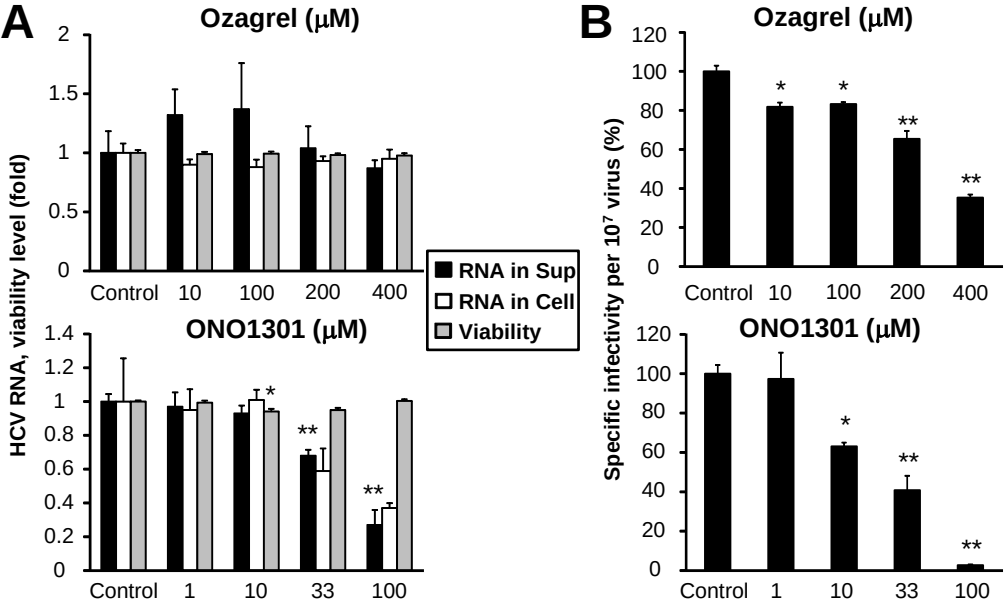
A
Ozagrel (μM)
HCV RNA, viability level (fold)
2
1.5
1
0.5
0
Control
10
100
200
400
RNA in Sup
RNA in Cell
Viability
ONO1301 (μM)
1.4
1.2
1
0.8
0.6
0.4
0.2
0
Control
1
10
33
100
B
Ozagrel (μM)
Specific infectivity per 10⁷ virus (%)
120
100
80
60
40
20
0
Control
10
100
200
400
ONO1301 (μM)
Control
1
10
33
100

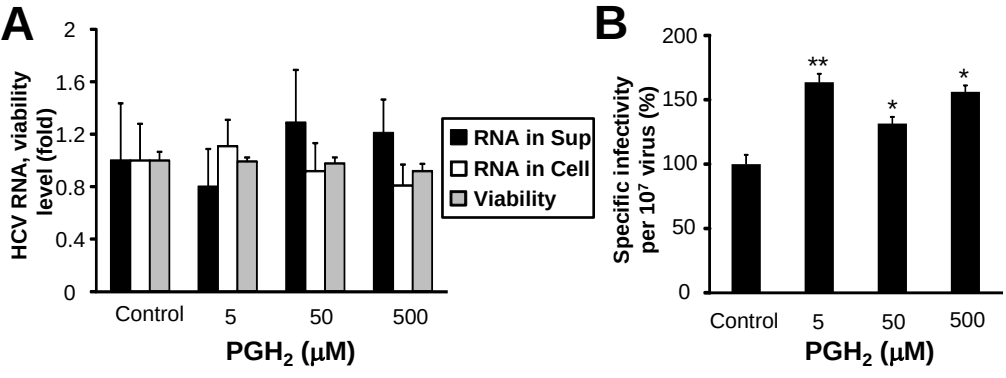
A
HCV RNA, viability level (fold)
2
1.6
1.2
0.8
0.4
0
RNA in Sup
RNA in Cell
Viability
Control
5
50
500
PGH2 (μM)
B
Specific infectivity per 10^7 virus (%)
200
150
100
50
0
**
*
*
Control
5
50
500
PGH2 (μM)

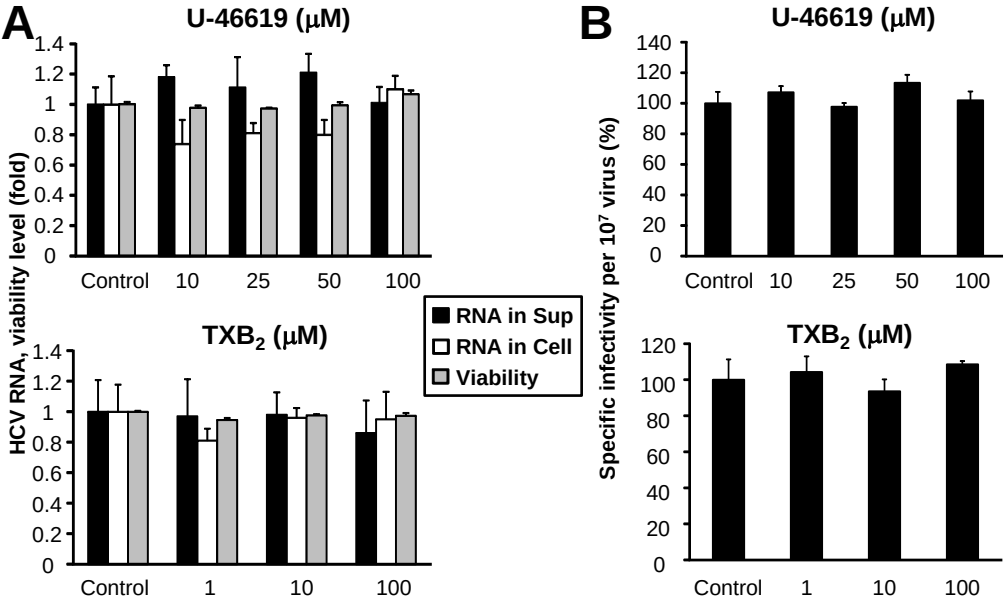
A
U-46619 (μM)
HCV RNA, viability level (fold)
1.4
1.2
1
0.8
0.6
0.4
0.2
0
Control
10
25
50
100
TXB2 (μM)
1
RNA in Sup
RNA in Cell
Viability
B
U-46619 (μM)
Specific infectivity per 10^7 virus (%)
140
120
100
80
60
40
20
TXB2 (μM)

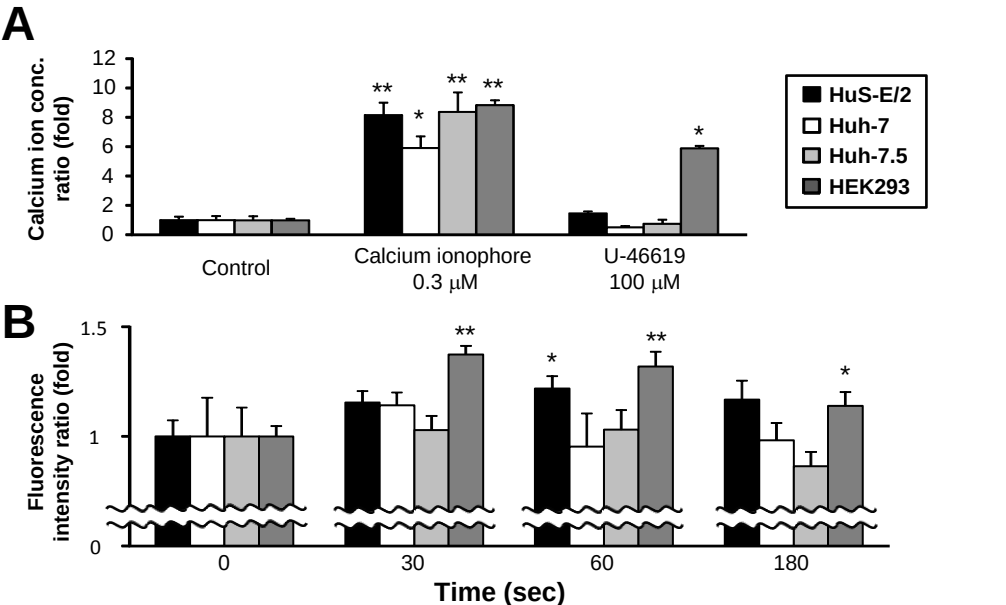
A
Calcium ion conc. ratio (fold)
12
10
8
6
4
2
0
**
*
**
**
*
HuS-E/2
Huh-7
Huh-7.5
HEK293
Control
Calcium ionophore 0.3 μM
U-46619 100 μM
B
Fluorescence intensity ratio (fold)
1.5
1
0
**
*
**
*
0
30
60
180
Time (sec)

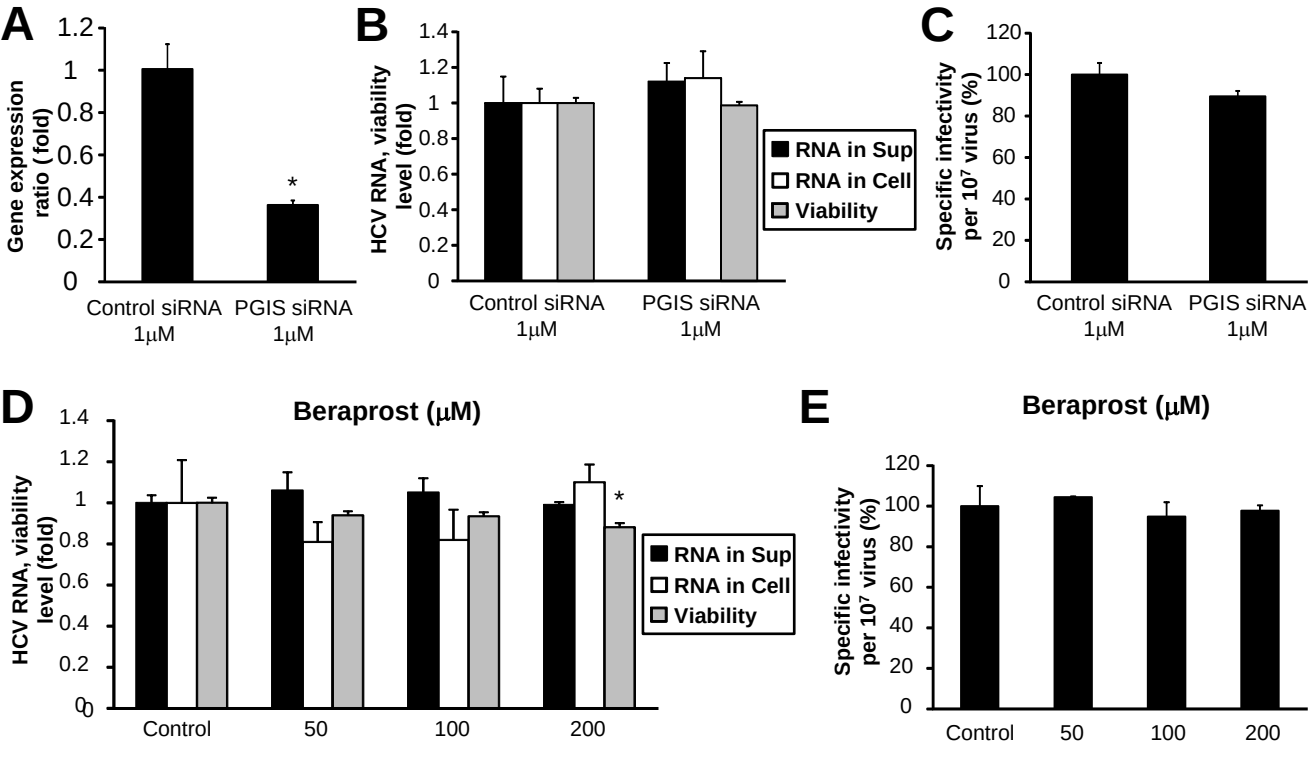
A
Gene expression ratio (fold)
1.2
1
0.8
0.6
0.4
0.2
0
*
Control siRNA 1μM
PGIS siRNA 1μM
B
HCV RNA, viability level (fold)
1.4
1.2
1
0.8
0.6
0.4
0.2
0
RNA in Sup
RNA in Cell
Viability
Control siRNA 1μM
PGIS siRNA 1μM
C
Specific infectivity per 10⁷ virus (%)
120
100
80
60
40
20
0
Control siRNA 1μM
PGIS siRNA 1μM
D
Beraprost (μM)
HCV RNA, viability level (fold)
1.4
1.2
1
0.8
0.6
0.4
0.2
0
*
RNA in Sup
RNA in Cell
Viability
Control
50
100
200
E
Beraprost (μM)
Specific infectivity per 10⁷ virus (%)
120
100
80
60
40
20
0
Control
50
100
200

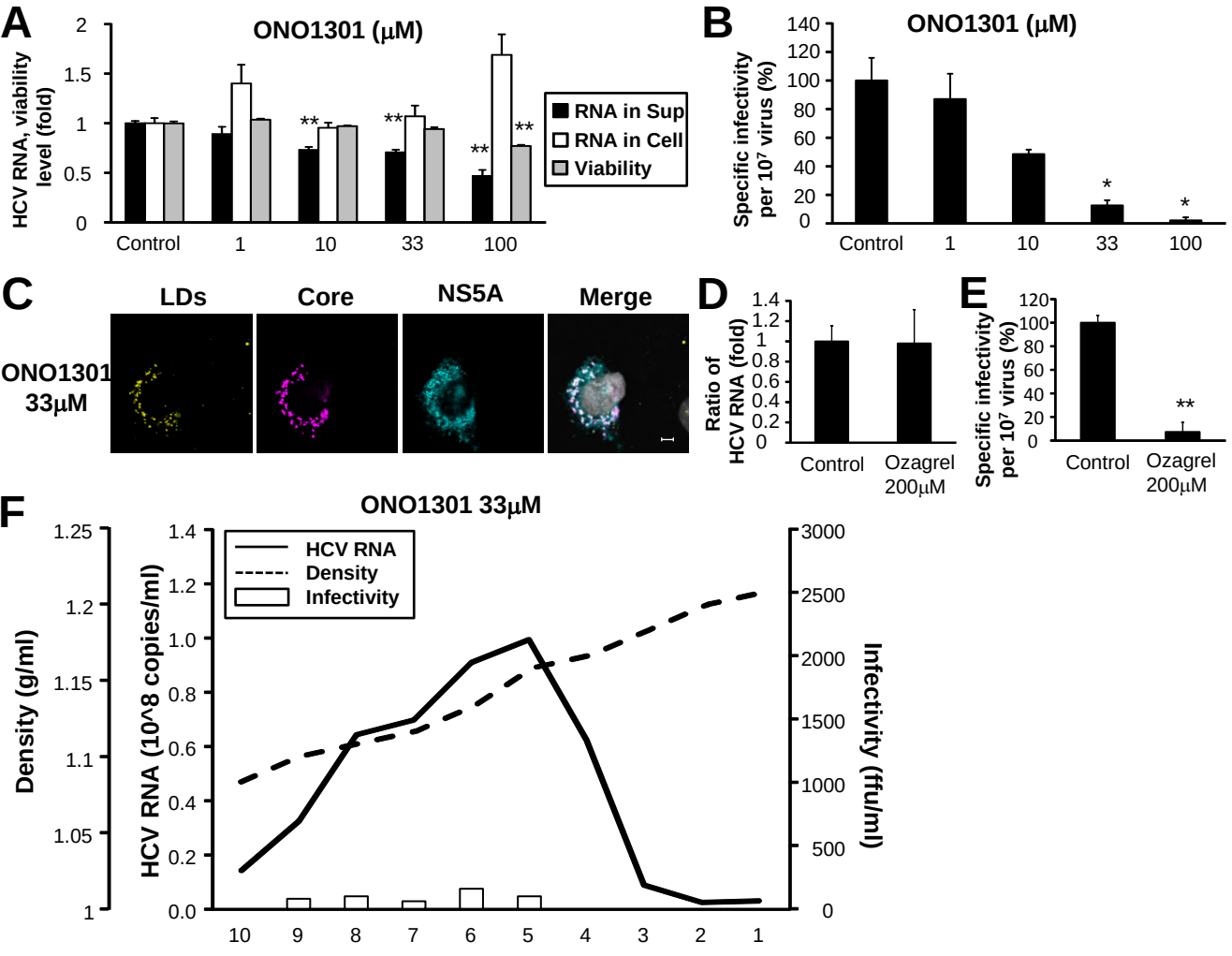
A
ONO1301 (μM)
HCV RNA, viability level (fold)
RNA in Sup
RNA in Cell
Viability
Control
1
10
33
100
B
ONO1301 (μM)
Specific infectivity per 10⁷ virus (%)
C
LDs
Core
NS5A
Merge
ONO1301 33μM
D
Ratio of HCV RNA (fold)
Control
Ozagrel 200μM
E
Specific infectivity per 10⁷ virus (%)
Control
Ozagrel 200μM
F
ONO1301 33μM
HCV RNA
Density
Infectivity
Density (g/ml)
HCV RNA (10^8 copies/ml)
Infectivity (ffu/ml)

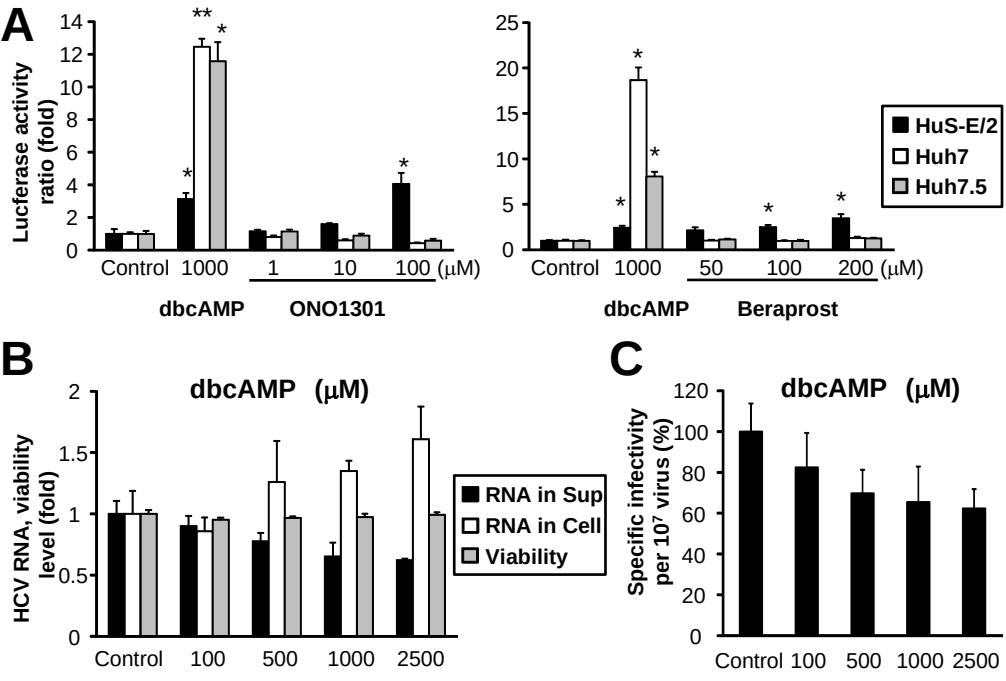
A
Lucferase activity ratio (fold)
14
12
10
8
6
4
2
0
**
*
*
*
Control
1000
1
10
100 (μM)
dbcAMP
ONO1301
25
20
15
10
5
0
*
*
*
*
*
Control
1000
50
100
200 (μM)
dbcAMP
Beraprost
HuS-E/2
Huh7
Huh7.5
B
dbcAMP (μM)
HCV RNA, viability level (fold)
2
1.5
1
0.5
0
Control
100
500
1000
2500
RNA in Sup
RNA in Cell
Viability
C
dbcAMP (μM)
Specific infectivity per 10⁷ virus (%)
120
100
80
60
40
20
0
Control
100
500
1000
2500

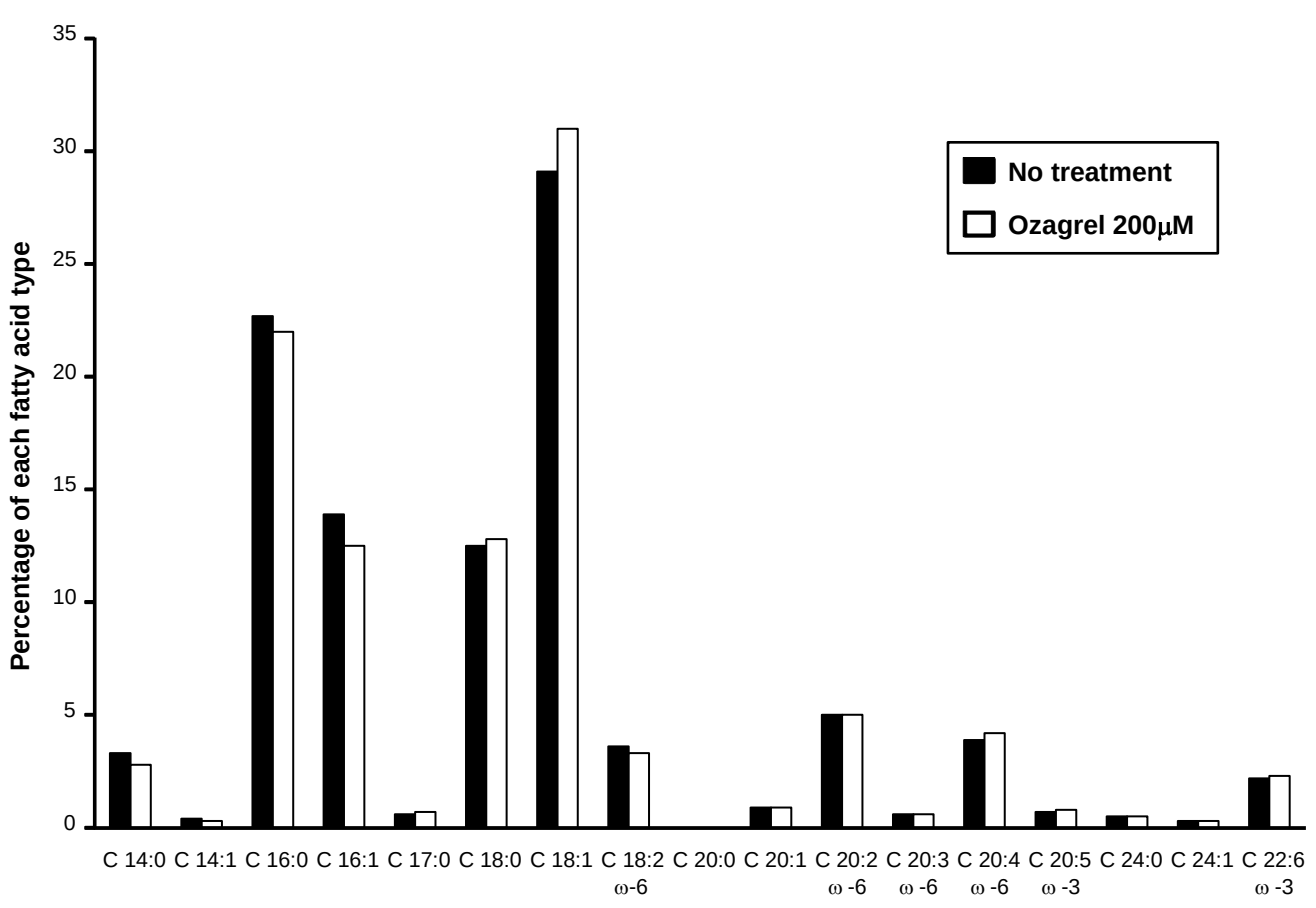
35
30
25
20
15
10
5
0
Percentage of each fatty acid type
No treatment
Ozagrel 200μM
C 14:0
C 14:1
C 16:0
C 16:1
C 17:0
C 18:0
C 18:1
C 18:2 ω-6
C 20:0
C 20:1
C 20:2 ω -6
C 20:3 ω -6
C 20:4 ω -6
C 20:5 ω -3
C 24:0
C 24:1
C 22:6 ω -3

HCV positive
Liver tissue

Human Mice

TP

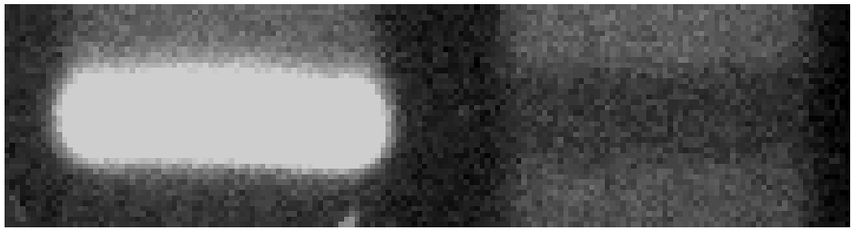

GAPDH

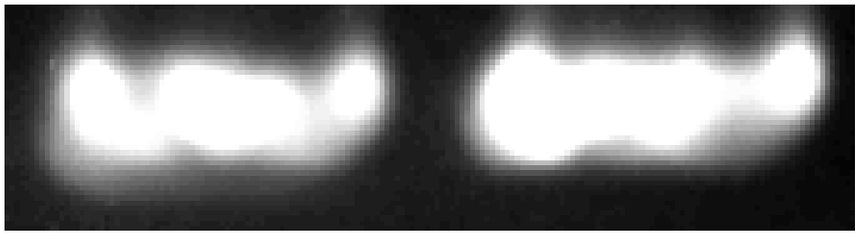

RT-
(GAPDH)

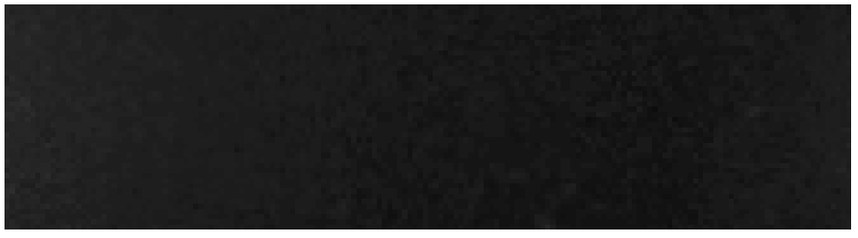

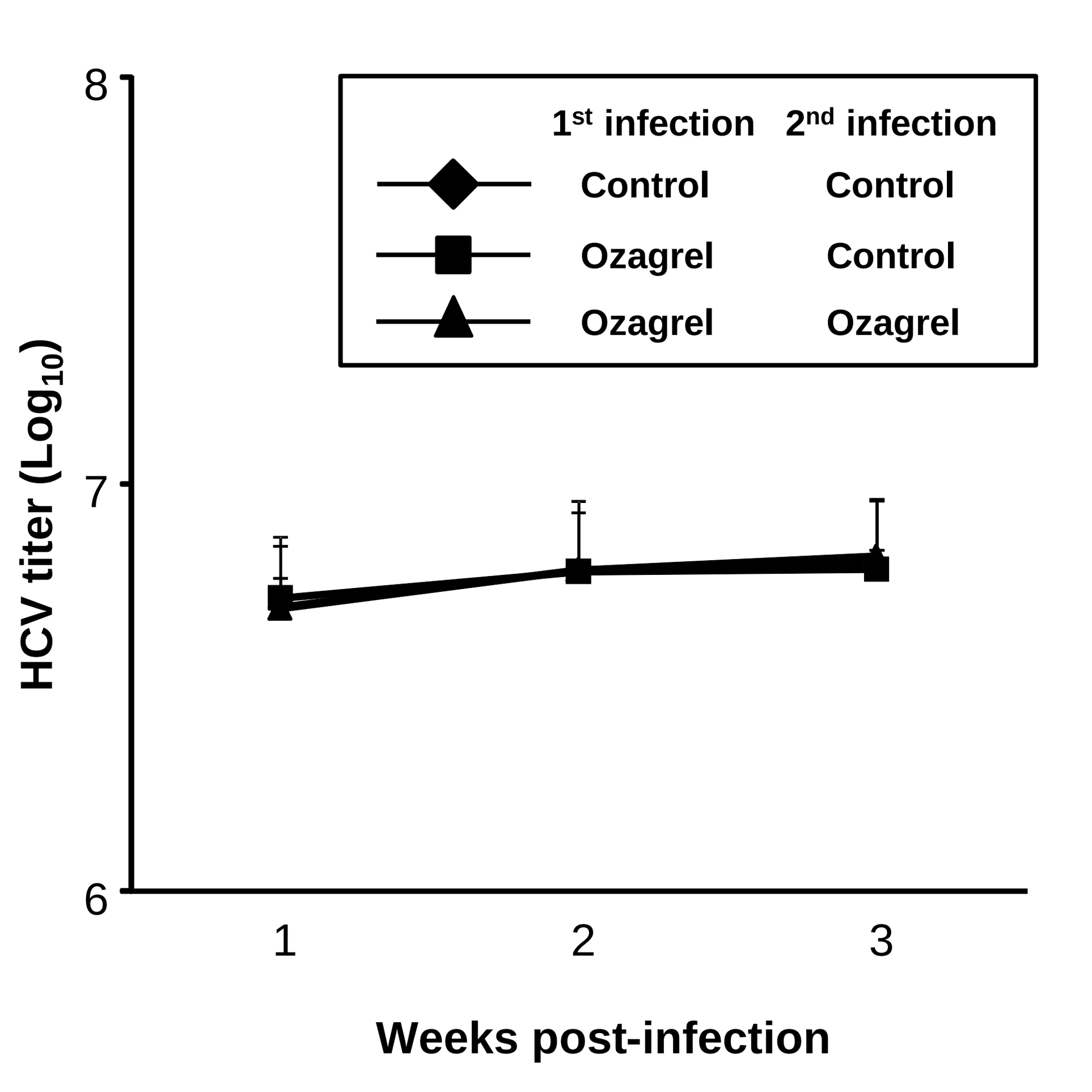
8
7
6
HCV titer (Log10)
1st infection
2nd infection
Control
Control
Ozagrel
Control
Ozagrel
Ozagrel
1
2
3
Weeks post-infection

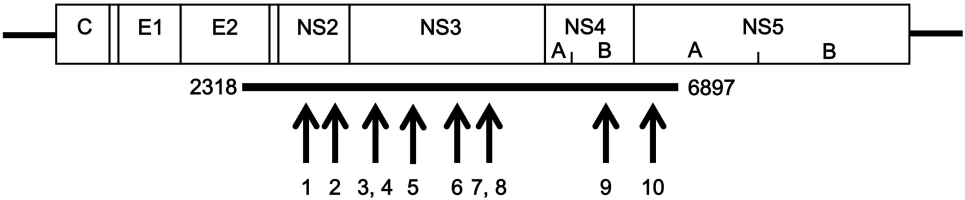

Number of substitution point	Position of nucleotide	Single base substitution	Amino acid replacement
1	3192	A→G	Asparagine→Aspartic acid
2	3264	A→G	Isoleucine→Valine
3 4	3596 3597	T→A C→T	Phenylalanine→Tyrosine
5	3859	C→T	Serine→Leucine
6	4283	G→A	Methionine→Isoleucine
7 8	4437 4439	G→A T→C	Glycine→Serine
9	5886	G→A	Valine→Methionine
10	6747	G→A	Alanine→Threonine

Genes	Primer Sequence 5'-3'	Product size (bp)	Annealing Temperture	Cycle
COX1	F: GCAGCTGAGTGGCTATTTCC R: ATCTCCCGAGACTCCCTGAT	324	60	32
COX2	F: GCAGTTGTTCCAGACAAGCA R: GGTCAATGGAAGCCTGTGAT	383	60	35
PGES	F: GAAGAAGGCCTTTGCCAAC R: GGAAGACCAGGAAGTGCATC	200	62	35
PGDS	F: AAGGCGGCGTTGTCCATGTGCAAGTC R: ATTGTTCCGTCATGCACTTATC	400	55	40
PGIS	F: TCCTGGACCCACACTCCTAC R: GCGAAAGGTGTGGAAGACAT	395	60	40
TXAS	F: TCTGCATCCCCAGACCTATC R: ATAGCCAGCGATGAGGAAGA	374	60	40
GAPDH	F: ATGGGGAAGGTGAAGGTCGG R: TGGAGGGATCTCGCTCCTGG	250	60	40
EP1	F: GGTATCATGGTGGTGTCGTG R: GGCCTCTGGTTGTGCTTAGA	324	60	40
EP2	F: AGGAGAGGGGAAAGGGTGT R: TCTTAATGAAATCCGACAACAGAG	267	60	40
EP3	F: GACAGTCACCTTTTCCTGCAAC R: AGGCGAACAGCTATTAAGAAGAAG	276	60	40
EP4	F: CAGGACATCTGAGGGCTGAC R: GTAGAAGGTCGTCTCCTTCTGCTC	269	60	40
DP	F: GCAACCTCTATGCGATGCAC R: GGGTCCACAATTGAAATCAC	292	60	32
IP	F: AAGACTGGAGAGCCCAGACC R: CCACGAACATCAGGGTGCTG	161	60	40
TP	F: CAGATGAGGTCTCTGAAGGTGTG R: CAGAGGAAGGTGAGGAAGGAG	304	60	40

Genes	Primer Sequence 5'-3'	Product Size (bp)
COX1	F: TCCGGTTCTTGCTGTTCCTG R: TCACACTGGTAGCGGTCAAG	151
PGES	F: CATCCTCTCCCTGGAAATCTCG R: CCGCTTCCTACTGTGACCC	129
PGDS	F: CCTGTCCACCTTGCACAGTC R: TCATGCTTCGGTTCAGGACG	123
PGIS	F: GCAGTGTCAAAAGTCGCCTG R: ACTCTCCAGCCATTTGCTCC	83
TXAS	F: TTTGCTTGGTTGCCTGTTCC R: CCAGAGTGGTGGTCTTCCAG	99
GAPDH	F: GACAGTCAGCCGCATCTTCT R: GCGCCCAATACGACCAAATC	104